Atomic Energy Control Board
P.O. Box 1046
Ottawa, Canada
K1P 5S9

Commission de contrôle de l'énergie atomique
C.P. 1046
Ottawa, Canada
K1P 5S9

INFO-0382

PROPAGATION MECHANISMS OF MOLTEN FUEL/MODERATOR INTERACTIONS

(AECB Project No.2.148.1)

by

D.L. Frost and G. Ciccarelli
McGill University

A research report prepared for the
Atomic Energy Control Board
Ottawa, Canada

Published June 1991

Canada

Research report

92-04389/

PROPAGATION MECHANISMS OF MOLTEN FUEL/MODERATOR INTERACTIONS

ABSTRACT

It is well known that a vapor explosion can result when molten metal is suddenly brought into contact with a cold volatile liquid such as water. However, the rapid melt fragmentation and heat transfer processes that occur during a propagating melt-water interaction are poorly understood. Experiments were carried out in the present work to investigate the fragmentation processes for single molten metal drops in water. To determine the time scale for the fragmentation of a drop, liquid metal drops (in thermal equilibrium with the water) as well as hot molten drops surrounded by a vapor film were subjected to underwater shocks with overpressures of up to about 20 MPa. In the hot molten drop tests, the induction time for the initiation of the explosion is typically less than 100 μs; at a corresponding time in the cold drop tests, very little or no direct hydrodynamic fragmentation of the drop has occurred. Therefore, in the hot drop case the fragmentation of the drop is dominated by thermal effects; i.e., the heat transfer from the melt to the water leads to violent boiling, pressurization, and drop fragmentation. The melt-water interaction consists of several cycles involving bubble growth and collapse. The strength of the interaction was not found to be a strong function of initial shock pressure (for molten tin drops with trigger pressures of up to 20 MPa), but depends on the thermal energy in the melt: high-temperature thermite drops generated a larger first bubble than lower temperature melt drops. A model for the fine fragmentation process for a hot drop is proposed that is based on thermal effects. The fragmentation processes governed by thermal effects observed in the present experiments are expected to play an important role in the *escalation* of a local interaction to a large-scale coherent vapor explosion, and are not accounted for in current transient models for propagating vapor explosions.

RÉSUMÉ

Il est bien connu que le contact soudain entre du métal en fusion et un liquide volatil froid comme l'eau peut causer une explosion de vapeur. Toutefois, on comprend encore mal les processus de fragmentation rapide de la matière en fusion et de transfert de chaleur qui interviennent lors d'une interaction propagatrice entre la matière en fusion et l'eau. Les

expériences relatées dans le présent document visent à examiner le processus de fragmentation lorsque des gouttes de métal en fusion sont introduites dans l'eau. On a déterminé l'échelle de temps pour la fragmentation d'une goutte en soumettant des gouttes de métal liquide (en équilibre thermique avec l'eau) ainsi que des gouttes de métal en fusion relativement chaud entourés d'un film de vapeur à des chocs sous-marins à des surpressions pouvant atteindre environ 20 MPa. Lors d'essais réalisés avec des gouttes de métal en fusion chaud, le temps d'induction menant au déclenchement de l'explosion est généralement inférieur à 100 μs; à un moment correspondant lors d'essais avec du métal liquide à la même température que l'eau, on observe très peu ou pas de fragmentation hydrodynamique directe de la goutte. Par conséquent, la fragmentation, dans le cas de la goutte de métal en fusion chaud, est dominée par des effets thermiques, c'est-à-dire que le transfert de chaleur du matériau en fusion à l'eau provoque un bouillonnement, une pressurisation et une fragmentation violents. L'interaction entre le matériau en fusion et l'eau consiste en plusieurs cycles d'expansion et d'affaissement de bulles. On a constaté que la force de l'interaction n'était pas une fonction importante de la pression initiale associée au choc (dans le cas de gouttes d'étain en fusion à des pressions de déclenchement pouvant atteindre 20 MPa), mais qu'elle dépendait de l'énergie thermique du matériau en fusion. Ainsi, des gouttes de thermite à haute température provoquaient une première bulle plus grosse que ne le faisaient des gouttes de métal à plus faible température. Le modèle proposé pour le processus de fragmentation fine est basé sur les effets thermiques. Les processus de fragmentation soumis aux effets thermiques et observés dans le cadre des présentes expériences devraient jouer un rôle important dans l'*accroissement* d'une interaction locale menant à une explosion de vapeur cohérente à grande échelle. Toutefois, les modèles provisoires courants de propagation des explosions de vapeur n'en tiennent pas compte.

DISCLAIMER

The Atomic Energy Control Board is not responsible for the accuracy of the statements made or opinions expressed in this publication and neither the Board nor the authors assume liability with respect to any damage or loss incurred as a result of the use made of the information contained in this publication.

TABLE OF CONTENTS

Page

ABSTRACT

RÉSUMÉ

1 INTRODUCTION 1

2 CURRENT STATUS OF PROPAGATION OF A VAPOR EXPLOSION 2

2.1 Previous Experimental Work 2
2.2 Effect of Confinement 3
2.3 Effect ofTrigger Strength 3
2.4 Thermal Detonation Model 4
2.5 Numerical Modelling of Propagation of a Vapor Explosion 5
2.6 Experiments on Hydrodynamic Fragmentation 7
2.7 Scope of Present Work 9

3 EXPERIMENTAL FACILITY 10

3.1 Drop Material 10
3.2 Apparatus 10

4. RESULTS AND DISCUSSION 12

4.1 Fragmentation of a cold drop 12
4.2 Fragmentation of a hot drop 13
4.3 Interaction of a shock with a hot solid sphere 14
4.4 Effect of trigger strength on explosion yield 15
4.5 Effect of melt thermal energy on explosion behavior 17
4.6 X-ray visualization of fragmentation process 18

5. CONCLUSIONS 20

ACKNOWLEDGEMENTS 22

REFERENCES 23

FIGURES 1 to 20

1 INTRODUCTION

It is well known that a vapor explosion can result when molten metal is suddenly brought into contact with a cold volatile liquid such as water. Mixing of the molten fuel and coolant produces a coarse fuel fragment-coolant mixture. Triggering of a local vapour explosion in this mixture and the subsequent propagation of a coherent vaporization wave through the mixture result in the formation of a high pressure steam bubble. Subsequent expansion of this high pressure steam bubble generates shock waves that would subject the structural surroundings to high hydraulic loadings.

In spite of the numerous experimental investigations (both laboratory and large-scale) as well as theoretical modelling, the basic propagation mechanisms of energetic vapor explosions are not well understood. In particular, it is not known what initial and boundary conditions, and triggering requirements are necessary to initiate and obtain self-sustained propagation of energetic vapor explosions. On a qualitative basis, it is known that vapor explosions can occur in both the volumetric coarse fragmentation mixture mode and in the stratified contact mode. However, the explosion limits (e.g., scale, confinement, and energetics of fuel-coolant mixture) and the triggering characteristics (e.g., amplitude and duration) have yet to be established. On a theoretical basis the detonation theory of Board, Hall, and Hall (1975) has not been verified experimentally and serious fundamental problems arise when the Chapman-Jouguet detonation theory for a homogeneous combustible gas is applied to a multiphase vapor explosion. Numerical codes that trace the propagation stage of a steam explosion include many simplifying assumptions and use fragmentation models that are not representative of the processes that occur in actual steam explosions. The results of the codes are not validated due to the lack of well-characterized experimental data.

A critical review of the current understanding of steam explosions was carried out as part of an earlier AECB sponsored work (Lee and Knystautas, 1987). It was concluded, on the basis of actual industrial accidents and large-scale experiments, that an energetic high yield steam explosion *cannot be regarded as an improbable event* if large quantities of molten fuel and coolant are mixed together. A subsequent AECB Contract (Lee et al., 1989) was carried out to provide an upper bound for the peak over-pressure and impulse generated during a postulated steam explosion involving the fuel contents of a single fuel channel. A conservative estimate of the pressure transients resulting from a steam explosion were calculated using a hydrodynamic shock wave code to model the expansion of the high

pressure vapor bubble. The model assumed *a priori* that a steam explosion occurs, i.e., a coarse mixture is formed followed by a coherent wave propagation. The critical conditions required for a coherent wave propagation and explosion were not considered in that contract. The dynamics of the propagation of a steam explosion were also not addressed in the previous contracts. As part of the present contract, small-scale experiments were carried out to investigate the fragmentation mechanisms that occur during the thermal explosion of single molten metal drops immersed in water. The information gained from the experiments would then be used to evaluate critically the analytical and numerical models that have been proposed to describe the propagation phase of a steam explosion.

To provide a context for the present experimental results, a brief review will be given of earlier work on the propagation stage of a steam explosion. In particular, earlier experimental work that observed a propagating interaction will be described, followed by a description of some analytical and numerical work that has attempted to model a propagating interaction. A key ingredient in the numerical models is the description of the fragmentation of the molten metal that occurs during a steam explosion. Since the fragmentation mechanism is strongly coupled with the propagation mechanism, a brief review of earlier work on hydrodynamic fragmentation will also be given. This will be followed by a presentation and discussion of the present experimental results.

2 CURRENT STATUS OF PROPAGATION OF A VAPOR EXPLOSION

2.1 Previous Experimental Work

Little is known regarding the propagation mechanisms of vapor explosions. Propagation refers to the progressive spatial development of the explosion process from a localized region where an interaction is first initiated, to the rest of the coarse mixture of the hot and cold liquids. Large scale tests (e.g., Mitchell et al., 1981) as well as small scale experiments (e.g., Fröhlich and Alisch, 1982; Baines, 1984; Fry and Robinson, 1979, 1980) have indicated a propagation process, although the propagation limits (i.e., the limiting conditions required to support the self-sustained propagation of a vapor explosion) have yet to be determined. Analogous to a combustion wave, it may be possible for different propagation regimes or modes to exist for the same liquid-liquid mixture,

depending on the initial and boundary conditions (e.g., thermodynamic conditions, mixture geometry, trigger amplitude, and degree of confinement).

For a stable coarse molten metal fragment-coolant mixture, a disturbance such as a shock wave is required to initiate a propagating energetic interaction. If the energy release in the reaction zone behind the leading shock wave is too slow, the shock will run ahead and will be *uncoupled* from the reaction zone. In this case, a propagating interaction (i.e., sequential explosion of the melt fragments) can still occur although the propagation speed will be less than the velocity of the leading shock. Such a propagation mechanism has been observed in earlier experiments at McGill for mixtures of molten metal and water (e.g., Frost and Ciccarelli, 1988). For propagation to occur in an array of melt fragments, a local explosion must generate a sufficient disturbance (e.g., the pressure waves and the hydrodynamic flow associated with the vapor bubble formed) to trigger the explosion of one or more of the adjacent fragments. For a given array of melt fragments, there must be a maximum spacing between the coarse fragments whereby the effects of the energy release due to the explosion of one cannot trigger an explosion of its immediate neighbors.

2.2 Effect of Confinement

The critical spacing between coarse fragments required to support a propagating interaction is a function of the degree of confinement of the mixture. For example, if a single drop is constrained to explode within a narrow channel, the maximum pressure and flow velocity associated with the motion of the vapor bubble are increased, effectively providing a stronger "trigger" for neighboring drops. Confining a coarse mixture to explode within a narrow channel simulates in some respects the effective confinement felt by an equivalent thin slab of coarse mixture within a larger volume. However, the channel walls impose a two-dimensional nature to the flow that differs from the three-dimensional flow that occurs during the explosion of a volume of coarse mixture. Therefore, although the qualitative effects of confinement on explosion propagation may be investigated at small scale, different propagation mechanisms may come into play at larger scale.

2.3 Effect of Trigger Strength

The effect of trigger strength on the initiation of a *propagating* explosion is poorly understood. For gas-phase detonations, it is well known for some gas mixtures that a weak initiation source can lead to detonation formation via an accelerating flame (gas

mixtures that detonate readily are often called "sensitive" mixtures), whereas for insensitive mixtures, a detonation can only be initiated directly by a strong initiation source. A similar situation may exist for steam explosions, although the criteria for a *sensitive* mixture have yet to be determined. Although a critical trigger strength may be required to initiate a steam explosion, the propagation mechanism of a *self-sustained* propagating explosion must ultimately be independent of the characteristics of the trigger source. In a propagating interaction, the energy release in the reaction zone behind the reaction front generates a pressure rise that drives the propagation of the front. The speed of propagation will depend on the rate of energy release within the reaction zone which in turn depends on the local mixture geometry, boundary conditions, and thermodynamic properties of the mixture. For a self-sustained propagating interaction, beyond some distance from the trigger source the initial triggering disturbance will no longer influence the propagation of the interaction. Therefore, for a steadily propagating front, the ability of the propagating interaction to sustain itself must depend only on the local coupling between the reaction zone and the front itself.

2.4 Thermal Detonation Model

A fast propagation mode has been proposed by Board et al., 1975 (and considered by others such as Sharon and Bankoff, 1981) in which the release of thermal energy is *coupled* to a leading shock wave, in analogy with a chemical detonation. In this propagation mode, shock-induced fragmentation of the dispersed molten fragments leads to rapid heat transfer to the coolant. If the timescale for energy release is sufficiently short, the pressure generated within the reaction zone would reinforce the strength of the propagating front. Board et al. calculated the conditions that would exist behind the explosion front by considering the wave structure as analogous to a chemical Chapman-Jouguet (CJ) detonation wavefront.

Fundamental problems arise when the classical CJ detonation theory for a homogeneous combustible gas is applied to a multiphase vapor explosion. In the classical detonation theory, a steady-state reaction zone is separated from a nonsteady expansion region by a plane (denoted the CJ plane) at which the flow velocity relative to the plane is sonic. The existence of this plane is necessary so that the expansion downstream cannot propagate upstream and affect the stability of the reaction zone and detonation front. For single phase flows, the conditions at the CJ plane can be determined by constructing a tangent to the Hugoniot curve from the original state. The Hugoniot curve represents the locus of

possible states on the pv diagram at the end of the reaction zone for a fixed energy release. This construction for calculating the CJ plane can be carried out formally for a molten metal-coolant mixture, but the resulting CJ point will not, in general, coincide with sonic flow for multiphase flow conditions. Additional problems arise because the assumption of thermal equilibrium at the CJ plane implies that fragmentation of the melt has been completed at this point. A nonequilibrium situation results if sonic flow occurs before velocity equilibration between the melt and coolant has been reached and hence before complete fragmentation and thermal equilibrium have occurred.

Estimation of the conditions that would exist behind a thermal detonation front does not imply that such a thermal detonation can actually be realized in practice. To demonstrate that a thermal detonation can occur, one must look at the rate at which the energy is deposited following the passage of the leading shock. This rate depends on how fast the fuel can be fragmented and hence transfer its heat to the coolant. Board et al. (1975) proposed that this could occur sufficiently fast through hydrodynamic fragmentation. Hydrodynamic fragmentation involves the breakup of the fuel due to the differential acceleration of the melt fragments and the surrounding coolant as a result of the passage of the shock. Velocity equilibration therefore implies termination of the fragmentation. The fragmentation mechanism plays a key role in determining the propagation mechanism and is an important ingredient in any model for the propagation phase of a vapor explosion. Current efforts at modelling the propagation phase will be discussed in the next section.

2.5 Numerical Modelling of Propagation of a Vapor Explosion

A number of techniques have been used to analyze the propagation phase of a vapor explosion. Application of classical detonation theory to vapor explosion propagation gives a prediction of the peak overpressure generated and propagation velocity but gives no insight into the physical processes that occur within the reaction zone itself. Bürger et al. (1986) supplemented the thermal detonation model with a detailed modelling of the melt fragmentation and rapid heat transfer processes that occur within the propagating wave. They considered the case in which high pressures are obtained in the reaction zone. For supercritical pressures (i.e., pressures greater than the critical pressure of water, or about 22.0 MPa), no vapor phase will be present and it is assumed that the melt fragmentation will be dominated by *hydrodynamic fragmentation* mechanisms. They considered fragmentation models based on drop deformation as well as those based on hydrodynamic instabilities at the surface of the drop. Two effects not considered include temperature

nonuniformities (i.e., heat transfer to only part of the coolant) and the effect of inert gas content. Bürger et al. (1986) applied the results of their code (FRADEMO) to compute the properties of steady-state thermal detonations for various melt-coolant mixtures, but did not consider the existence of such solutions which requires an understanding of the ability of a disturbance in a given mixture to escalate to the final state.

To investigate the escalation process by which a local disturbance grows to form a self-sustained coherent interaction, it is necessary to consider fragmentation mechanisms based on *thermal effects* that are expected to play a dominant role at low (subcritical) pressures. For example, following film collapse, rapid heat transfer can lead to rapid pressurization and vaporization which can directly fragment nearby melt fragments. A model based on thermal effects has been developed by Corradini (1981) and applied to single drop tests carried out at Sandia National Laboratories (Nelson and Duda, 1982). The model considers a local collapse of the vapor film surrounding a melt fragment (with possible jetting of the coolant into the melt) followed by rapid heat transfer and pressure build-up leading to fragmentation of the drop. Detailed experimental results are required to resolve the relative role of the various processes that occur during each stage of this model. A comprehensive model including both the escalation and steady-state propagation phases of a vapor explosion must consider fragmentation mechanisms due to thermal as well as hydrodynamic effects.

Another approach to analyzing the propagation stage of a vapor explosion is to solve the conservation equations for mass, momentum and energy directly using empirical correlations of hydrodynamic fragmentation to model the breakup of the melt fragments. This approach has been taken by Fletcher and Thyagaraja (1989) and Medhekar et al. (1988). With this approach the initial transient phase of a vapor explosion can be investigated as well as the sensitivity of the initial conditions on the characteristics of the propagation. However, one problem lies in the fact that there is not a sufficient amount of data on hydrodynamic fragmentation of liquid drops in a *liquid* medium. As a result, numerical modelers are dependent largely on data obtained for drop breakup in a gas medium. Furthermore, thermal effects are not considered to play a role in the fragmentation process in any of the current numerical codes. This is convenient for modelling because the fragmentation and heat transfer can be treated separately when in fact these two are coupled. The use of hydrodynamic fragmentation models alone will lead to unrealistic results, particularly for the initial escalation stage in which fragmentation due to thermal effects is expected to play a dominant role.

2.6 Experiments on Hydrodynamic Fragmentation

At this point it would be beneficial to survey some of the experimental data which is available concerning hydrodynamic fragmentation of liquid droplets in liquid and gas mediums. An review of this topic was done by Pilch, Erdman and Reynolds (1981). They identified five distinct fragmentation mechanisms. These mechanisms were classified in terms of the initial Weber number which is the main nondimensional parameter governing drop breakup (We = $\rho V^2 d/\sigma$, where ρ = density of the flow field, V = initial relative velocity between flow field and drop, d = initial drop diameter, and σ = surface tension of the drop). The five mechanisms are:

1. Vibrational Breakup	We < 12
2. Bag Breakup	12 < We < 50
3. Bag and Stamen Breakup	50 < We < 100
4. Sheet Stripping	100 < We < 350
5. Wave Crest Stripping followed by Catastrophic Breakup	350 < We

These fragmentation mechanisms are graphically illustrated in Fig. 1. In the postulated thermal detonation model, very large Weber numbers are expected (in excess of 350) and thus the *wave crest stripping followed by the catastrophic breakup* mechanism will play an important role. In this mechanism the windward side of the drop develops large-amplitude small-wavelength waves. The crests of these waves are continuously eroded by the flow over the drop. The stripped fragments are swept back into the drop's wake. This process is referred to as wave crest stripping. At later times the slower growing large wavelength waves grow (due to Rayleigh-Taylor instability of the upstream face of the drop), ultimately penetrating the drop and breaking it up into several large fragments. This is referred to as catastrophic breakup.

Reinecke and Waldman (1970) observed this wave crest stripping and catastrophic breakup in the breakup of water drops behind a strong shock wave in air. They also used flash x-rays in order to see through the mist produced by the wave crest stripping. In this way they obtained an empirical correlation for the drop mass time history given as follows

$$\frac{m}{m_o} = \frac{1}{2}\left[1 - \cos\left(\frac{\pi T}{T_b}\right)\right] \quad ,$$

$$T = \frac{Ut}{d}\left(\frac{\rho_m}{\rho_d}\right)^{1/2} \quad ,$$

where

m: = amount of mass stripped from drop

m_o = initial mass of drop

T = dimensionless time

T_b = dimensionless time for mass of drop to reduce to zero (breakup time)

U = flow velocity

t = dimensional time

d = initial drop diameter

ρ_m = density of the surrounding fluid

ρ_d = density of the drop

This correlation is used as a fragmentation model in some of the existing thermal detonation models. Reinecke and Waldman also proposed the following correlation for the time for the onset of catastrophic breakup as a function of the Weber number.

$$T_b = 45\ We^{-1/4}$$

Patel and Theofanous (1981) used regular photography to study the breakup of liquid drops in water. Their photographic results do not clearly demonstrate either the wave crest stripping or catastrophic breakup. Instead they observed that the drops exhibited a rapid and uniform blowup in all directions. They obtained the following fragmentation time versus Bond number correlation

$$T_b = 1.66\ Bo^{-1/4}$$

where $Bo = 3/8\ C_d\ We$, C_d = the drag coefficient,

and where they defined the drop breakup time to be when the drop expanded to twice its initial value.

Many different definitions have been proposed for breakup time. The variations in breakup time definitions and the difficulty in interpretation of experimental data make it difficult to compare results from different studies. Pilch et al. (1987) have reviewed the literature and found three characteristic times of interest: initiation of breakup, primary breakup and total breakup. The only data currently representing total breakup time for liquid-liquid systems is that of Baines and Buttery (1979). Their results showed no correlation with We with dimensionless complete breakup times ranging from 3 to 5.

2.7 Scope of Present Work

In order to study the coupling between the fragmentation and heat transfer one must do two simultaneous experiments; first, consider the fragmentation of a cold (or isothermal drop) where no thermal effects exist, then perform a second experiment under similar shock conditions with a hot drop of the same material. By comparing the induction time (time from when the shock wave reaches the drop to the onset of the explosive interaction) in the hot drop experiment to some characteristic fragmentation time in the isothermal drop experiment one can determine the influence of thermal effects on the fragmentation process. For example, if the induction time is longer than the fragmentation time then hydrodynamic fragmentation will play an important role. However, if the induction time is shorter this means that thermal effects dominate the fragmentation process for the explosion of the hot molten drop.

In the present study, experiments were carried out to test the fragmentation of liquid metal drops at the same temperature as the surrounding water (these tests are denoted *isothermal or cold drop tests*) as well as for high temperature molten metal drops. Fragmentation times were determined by visualizing the drop breakup with high-speed photography. The effect of trigger strength as well as melt temperature was considered. In each case, the peak triggering pressure was less than the critical pressure of water (about 22.0 MPa) so that the results are of relevance to fragmentation mechanisms in subcritical propagating steam explosions and the escalation phase of high-pressure steam explosions.

3 EXPERIMENTAL FACILITY

3.1 Drop Material

In the past there have been several different drop materials used in isothermal and hot drop experiments. For example Patel and Theofanous (1981) used mercury and gallium drops in a study of the fragmentation process in a hydrodynamic water shock tube. These are useful metals for isothermal drop experiments because they are liquid at or just above room temperature although they are toxic and tend to be fairly expensive. Many investigators have used tin for low temperature (< 1000°C) hot drop experiments. For high temperature melt-coolant experiments, thermitic melts have been most widely used (e.g., at Sandia National Laboratory and Winfrith). The drawback with tin and thermite is that they cannot be used in isothermal experiments. All of the above mentioned materials were used in the present experiments, but ideally one would like a safe inexpensive material that can be used both in isothermal and hot drop experiments. For this reason a low melting point alloy (T_{melt}= 49°C) consisting of 45% bismuth, 23% lead, 19% indium, 8% tin, and 5% cadmium (commercially called *cerrolow*) has also been used.

3.2 Apparatus

Two different facilities were used for the present experiments. Both consist of aluminum tanks, open at the top for delivery of the melt droplet, with an exploding wire for triggering mounted near the base of the tank. The trigger system consists in each case of an 8 μF capacitor which is charged to between 3 and 15 kV and discharged through a low-inductance circuit. During a trial, the discharge is initiated when the drop breaks a light beam from a low power He-Ne laser, causing a photodiode circuit to generate an electrical pulse. This pulse is then used, together with appropriate delay units, to fire the flash, camera shutter, and exploding wire sequentially. The trigger pressure is measured with the use of underwater pressure transducers placed in the water near the drop. Two types of pressure transducers are used: (1) an underwater tourmaline gauge (PCB Piezotronics 138A01, sensitivity 725 mV/MPa, quoted risetime of 1.5μs) and (2) an underwater PVDF pressure transducer (Imotec, sensitivity 11 mV/MPa, risetime 70 ns, sensitive diameter 0.5 mm). Signals from the tourmaline gauge are recorded with a PC-based data acquisition board operated at 1 MHz and from the PVDF gauge with a LeCroy 9400A oscilloscope recording at 30 MHz.

The first tank (18 cm x 18 cm x 27 cm high) is used for studying the effect of trigger strength on explosion yield. The interaction is recorded with a Cordin 16 mm rotating drum camera operated at 25,000 frames/s. The drop is illuminated from behind with the use of zirconium wire-filled flashbulbs (Sylvania FP-26) with a flash duration of 20-30 ms. The dropping mechanisms used in the hot and cold drop tests are shown schematically in Fig. 2. Each one consists of a hollow graphite cylinder with a plunger which when lifted allows the test drop to fall through. The plunger is a stainless steel rod with a K-type thermocouple mounted near the end to record the temperature of the drop prior to a trial. For the hot drop trials, the air gap between the graphite cylinder and the plunger is heated with a nichrome heating coil. For the cold drop experiments, the drop is submerged in the water at a temperature maintained above the melting point of the drop material. For the thermite mixture only a graphite cylinder is used with a piece of tape and paper covering the bottom of the cylinder to hold the mixture. The mixture is ignited by a propane torch flame directed on the top of the cylinder or with a nichrome wire embedded in the thermite.

An example of the pressure generated at the drop location by the exploding wire trigger system is shown in Fig. 3 for a charging voltage of 12 kV. The first spike on the lower trace (scale is 20 μs/div) represents the noise from the discharge, and the blast wave arrives at the drop location about 60 μs later, corresponding to a drop-electrode distance of 9 cm (the upper trace shows the blast wave expanded on a scale of 5 μs/div). The peak pressure of the shock wave is 12.7 MPa with a duration of about 5 μs and the second pressure pulse, that arrives at the drop about 70μs later, represents the reflected wave from the base of the tank. Following the arrival of the shock at the drop location, the pressure in the water actually drops below the ambient pressure and cavitation bubbles are formed. The cavitation bubbles are present for about 400 μs obscuring the photography during this time. Following the discharge of the capacitor and generation of the blast wave a vapor bubble is formed which expands pushing the water ahead of it. Therefore, the drop is first subjected to a flow of water generated from the shock which lasts about 5-10 μs and then to the flow associated with the expanding vapor bubble which can last up to several milliseconds.

The second tank is used for simultaneous flash x-ray and visual observation of the explosion. The width of the tank is 10 cm, optimized for best contrast on the x-ray film, and lexan windows are used for the x-ray photographs to minimize absorption of the x-rays. A Scandiflash 30 kV single head x-ray system generates soft x-rays with an exposure duration of 35 ns. Regular photography is taken in a direction perpendicular to the x-ray radiographs using the Cordin camera and a xenon flash-tube (duration of flash: 10

ms) for lighting. In this tank the exploding wire is recessed in a cylinder (6.4 cm diameter, 7 cm deep) so that the pressure recorded at the drop location (shown in Fig. 4 for a charging voltage of 7 kV) consists of several pressure pulses due to reflections from the base and sides of the cylinder. One of the reflected pulses has an amplitude that is higher (11.4 MPa) than the initial shock wave from the discharge. The oven used for heating the drop consists of a semicylindrical ceramic oven and a plunger system, similar to the one described above, is used for dropping the drop. The fall distance from the drop to the surface of the water is about 4 cm.

4 RESULTS AND DISCUSSION

4.1 Fragmentation of a cold drop

To determine the relative importance of hydrodynamic and thermal fragmentation effects, experiments were first carried out to subject a cold liquid metal drop (i.e., at the same temperature as the surrounding water) to a blast wave. In this case, since the drop and coolant form an isothermal system, only hydrodynamic effects can play a role in the breakup of the drop. The fragmentation process is best illustrated by considering the high-speed film record of a representative trial. Figure 5 shows a series of single frames taken from the photographic record for a trial with a 0.4 g drop of cerrolow alloy. The water temperature is 60°C so that the alloy drop remains a liquid at all times. The photographs illustrate the fragmentation of the drop following the passage of the triggering shock wave moving in the upward direction with a peak overpressure of 9.2 MPa. The times shown are with respect to the initiation of the triggering shock (the transit time for the shock to reach the drop is 60 μs). The black bar on the left edge of each photograph is a piece of tape of tape fixed to the front window that serves to provide a reference vertical position. In the first few hundred microseconds after the trigger is initiated, cavitation bubbles form due to the sharp expansion tail of the blast wave. Once the cavitation bubbles clear we can clearly see the drop fragmentation process. The windward or upstream side of the drop (i.e., the bottom of the drop) becomes rough relative to the smooth appearance before the arrival of the shock. Mass appears to be stripped continuously from the drop surface and swept to the back of the drop, in the form of filaments or fine fragments.

The fine fragmentation process observed is similar to the wave crest stripping mode given by Pilch (1981) for We > 350, where We is the Weber number of the flow. The exploding

wire trigger system generates two effects: the initial shock wave that interacts with the drop (a 10.0 MPa shock generates a flow with a Weber number of about 460) and a variable convective flow generated by the expansion of the steam bubble produced following discharge of the capacitor. Note from Fig. 5 even after 2 ms, although the profile of the drop has expanded and fine fragments are visible downstream, that the "parent" drop appears to be largely intact. Although a quantitative estimate of the degree of fragmentation as a function of time would require the use of flash x-ray visualization at each stage in the fragmentation process, it is clear that it takes many milliseconds to completely fragment a drop due to hydrodynamic fragmentation alone. In several films, at much later times (greater than 10 ms later), the drop fragments are visible and are spread over a large area. Since the drop remains liquid during the interaction, after the interaction the fragments tend to coalesce at the bottom of the tank. This makes it impossible to determine an accurate distribution of sizes of the fragments generated during the interaction.

4.2 Fragmentation of a hot drop

When a drop of molten tin or alloy, heated to 750°C is dropped into water and interacts with a triggering shock wave, the subsequent breakup of the drop has a different behavior than the breakup of a cold drop. The most dramatic difference is that the time for the fragmentation of a hot drop is an order of magnitude less than the corresponding value for a cold drop. Figure 6 illustrates the fragmentation process of a hot tin drop (initially at 750°C) that is subject to a triggering shock with a peak pressure of 6.0 MPa at the drop location. The drop itself has a flattened shape with an attached air bag that is formed when the drop first penetrates the water surface. At time t = 0 the exploding wire discharge is activated, illuminating the drop from below. After 60 μs the shock reaches the drop, and after an additional 60 μs the gas bag above the drop (and presumably also the thin vapor film surrounding the drop) has collapsed to a small size. Note that the air bag collapses symmetrically so that a reentrant water jet is *not* formed. 100 μs after the shock arrives at the drop, the first expansion of the steam bubble around the drop is apparent. The steam explosion bubble grows rapidly radially and reaches a maximum diameter after about 700 μs. Then it collapses to a minimum size after about 1.5 ms and then rebounds again to a second maximum at about 3.5 ms. This multiple oscillation of the steam bubble is characteristic of all the trials with molten tin drops. The second bubble maximum is usually larger than the first bubble maximum. Note that as the first bubble collapses, tin fragments remain in the water and appear dispersed over a large area.

In trials with hot tin drops at temperatures of less than 750°C, a thin curved cap of metal (typically representing less than 10% of the initial drop mass) often solidifies near the bottom of the drop during the explosion and is recovered after the trial. The outside of the cap usually has a rough, dull appearance, suggesting a relatively slow solidification. Whereas the interior of the cap is invariably smooth indicating a rapid freezing of the entire surface. The presence of the thin cap during a trial is evident from the high-speed film records in frames following the collapse of the first steam explosion bubble. For the higher temperature melts (tin above 750°C and thermite melts), complete fragmentation of the drop was observed in the majority of trials.

A comparison of Figs. 5 and 6 demonstrates that the purely hydrodynamic fragmentation mechanism cannot account for the fragmentation of the hot tin drop. The thermal energy associated with the hot drop must play a dominant role in the fragmentation process. It may be argued that the collapse of the large gas bag above the drop may generate hydrodynamic fragmentation of the drop due to the violent contact between the water and the drop. To test this hypothesis, it is necessary to remove the gas bag and observe the explosion of a drop that is initially surrounded only by a thin vapor film. The air bag attached to the drop also varies in size and shape randomly from one trial to the next and hence it represents another variable that is difficult to control.

To eliminate the gas bag, a funnel was placed in the water so that the passage of the drop through the funnel was such that the bag was dislodged. In this way, more repeatable initial conditions for the drop could be attained. Figure 7 shows the explosion of a 0.5 g tin drop subject to a triggering shock of 13.1 MPa. The tip of the funnel is visible near the top of each of the frames. The characteristic features of the explosion process are similar for the drops shown in Figs. 6 and 7, i.e., the presence of a gas bag does not significantly change the fragmentation process. Hence hydrodynamic fragmentation caused by collapse of the air bag plays little role in the fragmentation process.

4.3 Interaction of a shock with a hot solid sphere

To investigate the influence of melt fragmentation on the initial explosion and size of the first bubble maximum, experiments were carried out in a system in which no fragmentation was possible. In particular, a solid steel sphere with the same diameter (5 mm) and initial temperature (750°C) as the molten tin drops, was dropped into water and subjected to the same triggering shock conditions. Figure 8 shows an example of a solid hot sphere

interacting with a shock with a peak pressure of 4.3 MPa. The growth of the vapor bubble around the drop, estimated from the photos, is shown in Fig. 9. After the shock passes the drop, the vapor film surrounding the sphere collapses and a steam bubble is generated that grows to a maximum diameter about 500 μs later. The presence of a small bubble of gas or vapor on the top of the sphere (visible in the photograph at time t = 0), leads to an asymmetry in the bubble shape. The cavitation of the water in the tank generated by the passage of the triggering blast wave is most intense in the wake of the sphere because of the hot wake region of the sphere itself. When the steam bubble collapses, it collapses asymmetrically and appears to *peel* away from the drop from the bottom. This effect is due to the vertical convective flow generated by the steam bubble associated with the exploding wire trigger at the base of the tank. Note that after collapsing, the bubble rebounds slightly then disappears after about 1 ms. In the absence of fragmentation, the heat due to conduction from the center of the drop to the surface is insufficient to form a second steam bubble.

For a hot solid sphere, most of the thermal energy contained near the surface of the sphere is transferred following the initial collapse of the vapor film surrounding the sphere. The steam bubble that is generated grows to a maximum size in a similar time as that for a molten drop, although the maximum bubble diameter attained is slightly smaller. The similarity in the dynamics of the first bubble generated between a molten drop and solid sphere suggests that the energy transfer is limited to a thin surface layer of the drop and that significant fragmentation of the molten drop does *not* take place during the short time that the water is in contact with the drop prior to the expansion of the first bubble.

4.4 Effect of trigger strength on explosion yield

The size of the steam bubble generated during the interaction can be used as a measure of the yield of the explosion. For molten tin drops, the explosion usually occurs in two steps and two bubbles are generated successively. For thermite it is found that usually only one bubble is observed. Strictly speaking the second or the maximum bubble should be used to characterize the yield. The first bubble characterizes the intermediate stage of the fragmentation process initiated by the triggering shock. A series of experiments was carried out with 0.5 g tin drops initially at 750°C and subjected to triggering shocks with peak pressures ranging from 6 to 17.8 MPa. Figure 10 shows the growth of the steam bubbles generated during an explosion of a drop (with no attached gas bag) for four trials with different triggering pressures. It can be seen that the overall bubble oscillation

behavior is not a strong function of the triggering pressure over the range of trigger pressures studied and so in this case the triggering pressure plays little role in both first and second bubble dynamics and serves only to initiate the explosion process.

Figure 11 shows a compilation from experiments with both molten tin drops and solid spheres, illustrating the variation in the first bubble maximum (scaled by the effective drop diameter, D_o = 5.1 mm) estimated from the high-speed film record from each trial as a function of triggering pressure. The molten tin drop trials are distinguished depending on whether or not a gas bag is attached to the drop when the explosion is initiated. For drops with an initial gas bag present, above a threshold pressure of about 2.0 MPa, the size of the first bubble is D/Do ≈ 4 and does not vary significantly with trigger pressure. For drops without an attached gas bag, the first bubble maximum is usually slightly less than the values obtained for drops with attached bags. This may be due to the insulating effect of the gas bag as the drop falls in the water, reducing the heat loss from drops with a bag relative to a drop that is only surrounded by a thin vapor film. Thus the drop temperature is higher (for a drop with an attached bag) when the explosion process is initiated by the triggering shock. Also the gas bag itself may contribute to the volume of the first bubble and thus increase the total volume when compared to the case without the gas bag. For the solid sphere trials, the steam bubble generated is smaller (D/Do ≈ 2), but above a threshold pressure, the bubble size is not dependent on trigger pressure.

The bubble volume associated with the first bubble maximum is a measure of the expansion work done during the first interaction and is plotted as a function of triggering pressure in Fig. 12. The curves shown are second order polynomial fits to the data and indicate that the bubble volume approaches an asymptotic value that is not dependent on trigger pressure. Berman and Beck (1989) used the product of pressure and impulse as a measure of trigger strength. The volume at the first bubble maximum is replotted as a function of the PI product in Fig. 13 (the peak pressure and impulse for each data point shown was calculated using pressure traces obtained with a tourmaline-type transducer). The figure shows that the expansion work done by the first bubble is not significantly dependent on PI (up to a value of PI ≈ 3.5 MPa-kPa-s), above a threshold value of about PI ≈ 0.5 MPa-kPa-s.

For molten tin drops, the second bubble oscillation is always more violent than the first. Figure 14 shows the first and second bubble maxima, for drops without initial gas bags, as a function of trigger pressure. Although the first bubble maximum appears to have a weak

dependence on trigger strength, the second bubble maximum shows no significant dependence on trigger strength. The data in Fig. 14 can then be used to estimate the efficiency of each explosion, defined as the ratio of the expansion work done with the thermal energy available, i.e., efficiency = $p\Delta V/m(c_v\Delta T + h_{fusion})$. The results are shown in Fig. 15. The yield for the second explosion is typically about 2% of the *initial* available thermal energy.

4.5 Effect of melt thermal energy on explosion behavior

Figure 16 shows the bubble growth as a function of time showing the effect of the initial thermal energy of the drop. The trigger pressure for each trial fell within the range of 40-6.0 MPa. The initial mass of the tin drops was 0.5 g and the thermite drop (consisting of a mixture of Fe and Al_2O_3) is estimated to be 0.7 g. As the thermal energy of the melt drop increases, the strength of the first interaction (measured by the size of the steam bubble generated) increases. However, the strength of the second interaction does not correlate with thermal energy. For a tin drop at 420°C, most of the thermal energy is released in the first explosion so that upon collapse of the bubble the tin appears solidified and a second interaction does not occur. For tin drops at 750°C, the second interaction is always larger than the first, and in fact the second bubble is even larger than the steam bubble generated with the thermite drop. The high-temperature thermite drop interaction is shown in Fig. 17. At time t = 0, the thermite drop is visible near the bottom of each frame, surrounded by a large gas bag. A bubble of noncondensible gas is visible in the upper part of each photograph. During the explosion of the thermite drop, a large fraction of the thermal energy is released in the first interaction so that the second bubble produced has the same size as the first (see Fig. 16). The large amount of noncondensible gas initially surrounding the thermite drop also serves to impede the collapse of the steam bubble generated and limit the size of the second interaction.

The effect of initial temperature on the interaction with a solid sphere is shown in Fig. 18. Increasing the initial thermal energy of the sphere increases only slightly the size of the steam bubble generated following the interaction with the shock. Although at higher temperature the internal energy is higher but rapid formation of vapor drives the water from the hot steel surface so that the effective total energy transfer is not increased significantly with higher steel ball temperature.

4.6 X-ray visualization of fragmentation process

To view the fragmentation of the melt drop itself during an explosion, it is necessary to use flash x-ray photography to "see" through the steam bubble generated. Figure 19 shows simultaneous x-ray and regular photographs during the explosion of 0.5 g tin drops. In each case, the drops were initially at 700°C and were subjected to a shock wave with a peak pressure between 5.0 and 6.0 MPa. The x-ray unit generates a single flash so that each x-ray photograph represents a different experiment. From the high-speed film record of each trial, the stage of the bubble growth process at the instant when the x-ray photograph was taken can be determined. The graph on the right side of Fig. 19 shows the timing of the x-ray photographs relative to the size of the steam bubble.

About 300 μs after the shock reaches the drop the steam bubble has grown to nearly twice the diameter of the original drop. At this time the drop is largely intact but the surface of the drop exhibits a fuzzy appearance indicating fine-scale fragmentation. After 700 μs, the steam bubble is nearing its maximum diameter. At this time, the profile of the drop has expanded considerably and thin "fingers" of tin extend from the drop. Fine tin fragments are also evident near the bubble surface. At 1.48 ms, just *prior* to the collapse of the first steam bubble, the drop appears to be finely fragmented and spread over a large area.

The x-ray photographs illustrate several features of the fragmentation process. After the passage of the shock, the subsequent violent film collapse itself does not significantly fragment the drop. The majority of the fragmentation (or dispersion) of the drop takes place during the expansion and collapse of the *first* steam explosion bubble. When the first bubble collapses, the water drawn in with the bubble contacts the highly dispersed drop and a second, more powerful interaction is generated due to the enhanced surface area of the drop.

Figure 20 shows a series of x-ray photographs of much larger 2.5 g tin drops, where better resolution can be obtained at the expense of some variation in the initial drop shape from one trial to the next due to the deformation of the drop that occurs as the drop falls through the water. The temperature of each drop is initially 600°C. A gas bag is attached initially to each drop (it is clearly visible in frame A, taken just before the shock arrives at the drop). Although simultaneous high-speed photographs were not taken during these trials, the characteristic bubble growth behavior (shown inset in Fig. 20) was reconstructed using the high-speed films of the explosion of other 2.5 g drop trials. At early times, fine filaments

of tin are visible at the periphery of the drop (for example, see picture D, taken at 500 μs). The x-ray photograph taken at 1.5 ms demonstrates that the drop is highly fragmented *before* the collapse of the first bubble. The diameter of the steam bubble in picture H is roughly the same as the diameter of the tin fragments. The fact that the area between the tin fragments has a light grey shade suggests that the steam bubble contains a significant proportion of water, probably in the form of fine droplets (a bubble of vapor only with this diameter appears white on an x-ray photograph). Subsequent vaporization of these superheated water droplets contribute to the explosive yield as characterized by the volume of the second bubble.

The x-ray photographs clearly demonstrate that surface fragmentation of the drop is occurring as the first vapor bubble is expanding. At the maximum size of the first bubble the x-ray photographs indicate that a significant fragmentation has occurred (e.g., see Fig. 20, photographs G and H). A plausible mechanism of this fragmentation process is the impingement of the two-phase jet on the drop surface as the vaporization front propagates into the superheated water as the first bubble is expanding. In the recent experiments of Hill and Sturtevant (1990), where a superheated column of freon is suddenly depressurized, a vaporization front is observed to propagate into the superheated fluid. In the wake of the front is a two-phase jet of liquid droplets as well as vapor (similar two-phase jets produced during the rapid evaporation of a superheated column of liquid have also been observed by Chavez et al., 1985). The fluid droplets are torn off the interface due to the growth of surface instability. In the present problem the collapse of the vapor film induced by the triggering shock brings about liquid-liquid contact between the water and the hot drop surface. The superheated water surrounding the drop subsequently vaporizes with the growth of the first bubble. The vaporization front then recedes back into the water and in the wake of this front, the two-phase jet (similar to Hill's observation) then penetrates into the hot drop. The water droplets embed themselves and receive a high degree of superheat. Their subsequent expansion results in the fine fragmentation of the drop during the first bubble growth as indicated by the x-ray photographs. In this manner the fragmentation is derived from the thermal energy of the drop with little dependence on the triggering strength.

The triggering shock perhaps influences the duration of the liquid-liquid contact and hence the degree of superheat of the water attained prior to the first bubble growth. The convective flow of the water set up by the triggering shock also plays a role in the subsequent dynamics of the first bubble growth as can be observed in the present

photographic records. From the high density of the vapor inside the first bubble as shown in the x-ray records (e.g., Fig. 20H) and the debris of the fragmented tin drop, the collapse of the first bubble is impeded and is not as described by Rayleigh theory. Thus the fragmented tin that is dispersed within the first bubble is not recompressed as the first bubble collapses. This is also evident in the photographic records of the present experiments.

5 CONCLUSIONS

The present study was carried out to investigate the fragmentation mechanism of single melt drops and the role of trigger strength and drop temperature. The peak pressure and impulse at the drop location were varied up to maximum values of about 20 MPa and 3.4 MPa-kPa-s, respectively. For cold liquid metal drops, fragmentation of the drop occurs over a long timescale (the bulk of the drop is still intact after 2 ms) as mass is stripped off the surface of the drop. For hot drops, the induction time for the initiation of the explosion is typically less than 100 μs. For tin drops, the explosion process consists of two steps, with the second bubble generated usually larger than the first. For drops with an attached gas bag, a trigger threshold (a peak pressure of 2 MPa or a PI product of about 0.5 MPa-kPa-s) was required to fully collapse the vapor/gas film and initiate a violent interaction. For drops with no attached gas bag, there was a weak dependence on trigger pressure of the first bubble maximum. However, the size of the second bubble maximum showed no dependence on trigger strength. For molten tin drops at 750°C, the efficiency of the second bubble interaction (as measured by the ratio of expansion work done to thermal energy available) varied from 1 to 7 %. Increasing the thermal energy of the drop resulted in a larger bubble generated in the first interaction although the overall explosion yield was not directly related to drop temperature.

The results of the present study show, over the range of trigger strengths tested, that the fragmentation of a hot molten drop is *not* governed by the so-called hydrodynamic fragmentation model that is widely used in numerical studies of the thermal detonation problem. In this model, the fragmentation process is due to the growth of surface instability associated with the relative velocity between the drop and the surrounding coolant with the thermal energy playing a minor role if at all. In this model the fragmentation process (rate) depends directly on the triggering strength. The present results indicate a very weak dependence on the triggering strength and that the triggering

process serves only to collapse the vapor film and initiate the subsequent fragmentation process. In the present experiments, the energy that leads to the drop fragmentation is derived from the thermal energy of the melt itself, rather than that associated with direct shattering of the drop by the initial shock. Of course, this conclusion is only valid for pressure levels comparable to those attained in the present experiments (up to ~ 20 MPa). For much higher pressures (e.g., ~ 100 MPa) the production of vapor would be suppressed and in this case it is expected that hydrodynamic fragmentation processes would dominate. Detailed experiments are required at these pressure levels to determine if hydrodynamic fragmentation can occur sufficiently rapidly to fragment a drop prior to velocity equilibration between the flow and the drop (at which point hydrodynamic fragmentation ceases).

The above conclusions have important implications concerning the fragmentation models used in numerical codes for the propagation of a vapor explosion. The majority of models (see Fletcher and Anderson, 1990 for a recent review) for the fragmentation process are based on hydrodynamic fragmentation mechanisms (i.e., due to relative velocity between melt and coolant or Rayleigh-Taylor instability). One exception is the work of Oh and Corradini (1987) who considered a fragmentation model driven by film collapse. The codes based on hydrodynamic fragmentation do not consider the fact that thermal effects can lead to fragmentation as well. In the present experiment the hot drops fragment following film collapse and rapid boiling in a time scale much shorter than that associated with direct hydrodynamic fragmentation of the drops. It is likely in the initial *escalation* stage of a coherent vapor explosion, when system pressures are still relatively modest (i.e., $p < p_{crit} = 22.0$ MPa) that thermal fragmentation effects will dominate. Only at higher pressures will direct hydrodynamic fragmentation play an important role.

Simultaneous x-ray and regular photography indicate that fragmentation occurs subsequent to the film collapse and continues during the growth of the first vapor bubble. In fact significant fragmentation can occur during this first stage of bubble growth. A thermal fragmentation mechanism has been proposed in which the two-phase jet associated with the receding vaporization front into the superheated coolant plays a dominant role in the fragmentation process. The penetration of the hot drop and the subsequent expansion of the embedded fine superheated water droplets in the drop leads to dispersion of the melt drop. The present results are is accord with the model proposed by Buchanan (1974) as far as the general principle that the thermal energy of the hot drop provides the driving force for the fragmentation itself. The present proposed scheme differs in detail with Buchanan's

model in the mechanisms responsible for the production of the liquid jet that penetrate the hot drop. In Buchanan's model, the coolant jet(s) that penetrate(s) the drop is credited to the asymmetrical collapse of vapor bubble(s) formed when the triggering shock collapses the vapor film and brings about liquid-liquid contact. In the present proposed scheme, the two-phase liquid jet is associated with the instability of the vaporization front that recedes into the superheated liquid subsequent to film collapse and liquid-liquid contact. These two-phase jets from a vaporization front have been conclusively demonstrated by Hill and Sturtevant (1990). As in Buchanan's model, the present model utilizes the thermal energy of the drop for fragmentation instead of the energy from the triggering source. This is supported by the experimental evidence that the total yield is practically independent of the triggering strength. It is interesting to note the present experiments indicate that the dispersion of the fine fragments occurs during the first bubble growth cycle. The motion of the fine fragments thus occurs in a vapor phase medium with significantly less drag. Therefore the energy required for dispersion is significantly reduced permitting a more efficient dispersion process.

None of the current models for propagating vapor explosions can be applied to predict the results from an actual experiment with any degree of confidence. In practical situations, fuel-coolant mixtures are far from being homogeneous, and key assumptions in the codes (such as assuming that all of the coolant is heated uniformly) break down. Confidence in our ability to model propagating vapor explosions will not improve until more well-characterized experimental results are available to validate the essential physics that the codes are based on.

ACKNOWLEDGEMENTS

The authors would like to thank the following for their comments and for many stimulating discussions: Drs. A. Omar, V. Q. Tang, and Q. S. Truong of AECB; Prof. J. H. S. Lee of McGill University, Joe Shepherd of RPI; and Marshall Berman and his staff at Sandia National Laboratories (Dave Beck and Lloyd Nelson). Assistance with the experiments involving x-ray photography was provided by P. Watts and R. Katofsky. Financial support for the present study was provided by the Atomic Energy Control Board of Canada, the Natural Sciences and Engineering Research Council of Canada, and Sandia National Laboratories.

REFERENCES

Baines, M., "Preliminary measurements of steam explosion work yields in a constrained system," First U.K. National Conference on Heat Transfer, *Institution of Chemical Engineers Symposium Series*, No. 86, pp. 97-108, 1984.

Baines, M. and Buttery, N. E., "Differential velocity fragmentation in liquid-liquid systems," Report RD/B/N4643, Berkeley Nuclear Labs, UK, 1979.

Berman, M. and Beck, D., "Steam explosion triggering and propagation: hypothesis and evidence". To appear in *Proc. 3rd International Seminar on Containment of Nuclear Reactors*, University of California, Los Angeles, CA, 10-11 August, 1989. (Also available as Sandia National Laboratory Report: SAND89-1878C).

Board, S. J., Hall, R. W., and Hall, R. S., "Detonation of fuel coolant explosions," *Nature* 254, pp. 319-325, 1975.

Buchanan, D. J., "A model for fuel-coolant interactions". *J. Phys. D.*, App. Phys., 7, 1974.

Bürger, M., Carachalios, C., Kim, D. S., and Unger, H., "Theoretical investigations on the fragmentation of drops of melt with respect to the description of thermal detonations (vapor explosions) and their application in the code FRADEMO," *Commission of European Communities*, Report EUR 10660 EN, 1986.

Chaves, H., Lang, H., Meier, G. E. A., and Speckmann, H.-D., in *Lecture Notes in Physics: Flow of Real Fluids*, edited by G. E. A. Meier and F. Obermeier, Springer, Berlin, 115, 1985.

Corradini, M. L., "Phenomenological modeling of the triggering phase of small-scale steam explosion experiments," *Nucl. Sci. Eng.* 78, pp. 154-170, 1981.

Fletcher, D. F., and Thyagaraja, A., "A mathematical model of melt/water detonations," *Appl. Math. Modelling*, 13, pp. 339-347, 1989.

Fletcher, D. F. and Anderson, R. P., "A review of pressure-induced propagation models of the vapour explosion process". *Culham Laboratory report:* CLM-P879, (To appear in Progress in Nuclear Energy, 1990).

Fröhlich, G. and Alisch, S., "Optische Erfassung der Wechselwirkung von heissen Zinnschmelzestrahlen mit Wasser bei selbst und Stosswellentriggerung," Rep. IKE2-58, *Institut für Kernenergetik und Energie systeme*, Universität Stuttgart, Stuttgart, FRG, 1982.

Frost, D. L. & Ciccarelli, G. "Propagation of Explosive Boiling in Molten Tin-Water Mixtures", Proc. of *1988 ASME/AIChE National Heat Transfer Conference*, Houston, HTD-96, Vol. 2, pp. 539-548, 1988.

Fry, C. J. and Robinson, C. H., "Experimental Observations of Propagating Thermal Interactions in Melt/Water Systems," *Fourth CSNI Specialist Meeting on Fuel-Coolant Interaction in Nuclear Reactor Safety*, Bournemouth, UK, 1979.

Fry, C. J. and Robinson, C. H., "Results from Selected Experiments Performed in the Thermir Facility at AEE Winfrith," Atomic Energy Establishment, Winfrith, Dorchester, Dorset, 1980.

Hill, L. G. and Sturtevant, B., "An experimental study of evaporation waves in a superheated liquid". *Proc. IUTAM Symposium* Göttingen, Germany, 1989, 25-37, Springer-Verlag, Berlin, 1990.

Lee, J. H. S. and Knystautas, R., "Molten fuel-moderator interaction: an investigation of the potential for steam explosion," AECB Report INFO-0227, 1987.

Lee, J. H. S. et al., "Numerical computation of underwater explosions due to fuel-coolant interactions," AECB Report INFO-0312, 1989.

Medhekar, S., Abolfadl, M., and Theofanous, T. G., "Triggering and propagation of steam explosions," *Proc. ANS National Heat Transfer Conf.*, Houston, 24-27 July, 1988, 2, pp. 244-251, 1988.

Mitchell, D. E., Corradini, M. L., and Tarbell, "Intermediate Scale Steam Explosion Phenomena: Experiments and Analysis," SAND81-0124, Sandia National Laboratories, Albuquerque, N.M., 1981.

Nelson, L. S. and Duda, P. M., "Steam-explosion experiments with single drops of iron oxide melted with a CO_2 laser," *High Temperatures-High Pressures*, Vol. 14, pp. 259-281, 1982.

Oh, M. D. and Corradini, M. L., "A propagation/expansion model for large scale vapor explosions," *Nucl. Sci. Eng.* 95, pp. 225-240, 1987.

Patel, P.D. and Theofanous, T.G., "Hydrodynamic fragmentation of drops," *Journ. of Fluid Mech.*, Vol. 103, pp. 207-223, 1981.

Pilch, M., Erdman, C.A. and Reynolds, A.B., "Acceleration induced fragmentation of liquid drops," Prepared for the Nuclear regulatory Commission, NUREG/CR-2247, 1981.

Pilch, M. and Erdman, C. A., "Use of breakup time data and velocity history data to predict the maximum size of stable fragments for acceleration-induced breakup of a liquid drop," *Int. J. Multiphase Flow*, Vol. 13, No. 6, pp. 741-757, 1987.

Reinecke, W. G. and Waldman, G. D., "An investigation of water drop disintegration in the region behind strong shock waves," *Proc. 3rd Intl. Conf. on Rain Erosion and Associated Phenomena*, Vol. 2., 629-667, 1970.

Sharon, A. and Bankoff, S. G., "On the existence of steady supercritical plane thermal explosions," *Int. J. Heat Mass Transfer* 24, pp. 1561-1572, 1981.

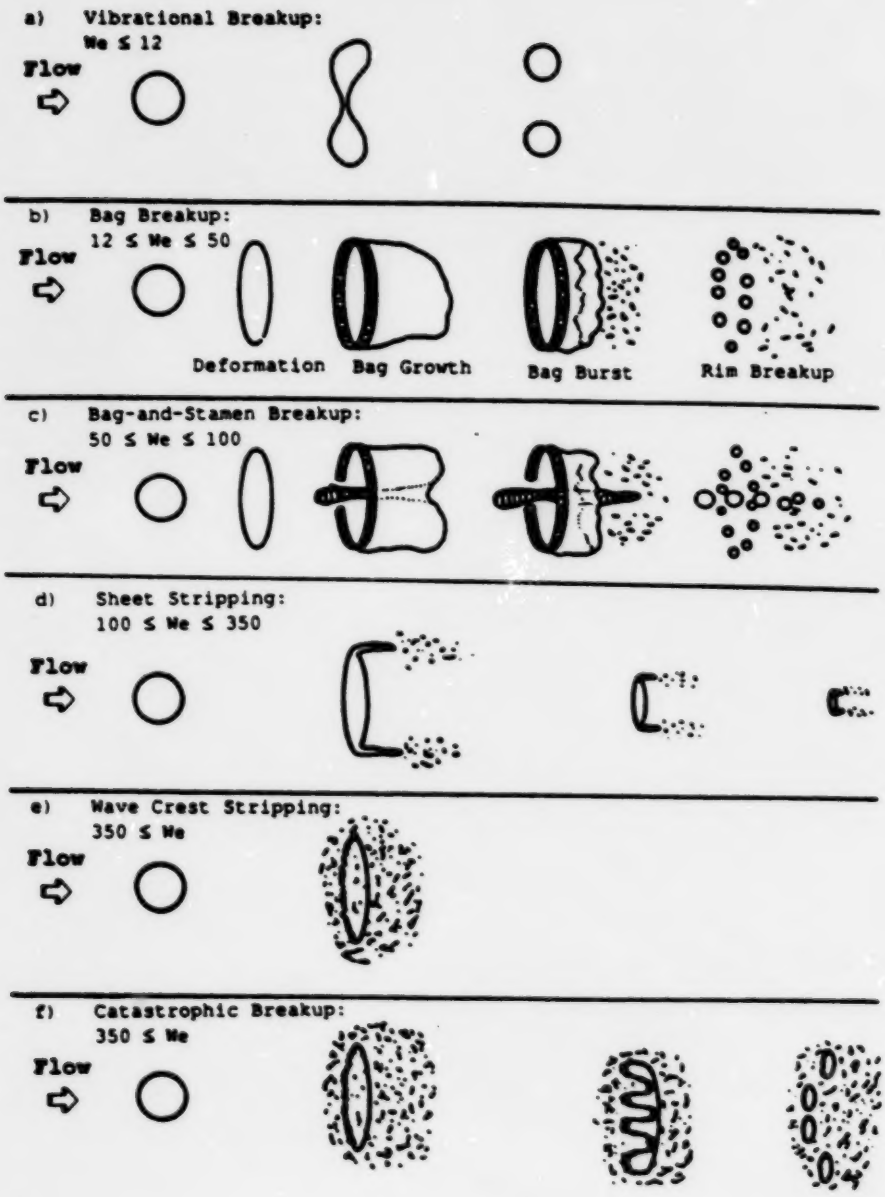

Fig. 1 Fragmentation of a drop as a function of Weber Number (taken from Pilch et al., 1981)

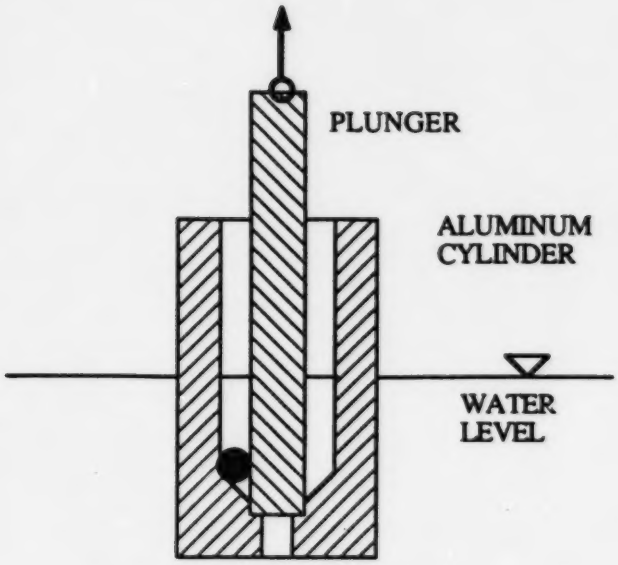

ISOTHERMAL DROP DROPPER

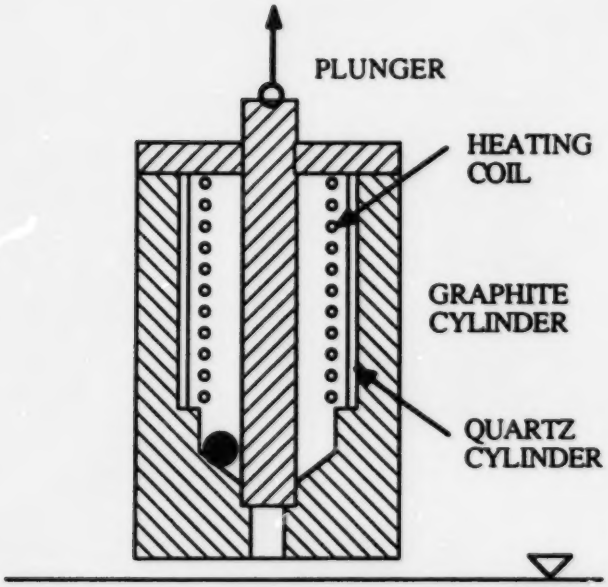

HOT DROP DROPPER

Fig. 2 Dropping mechanisms

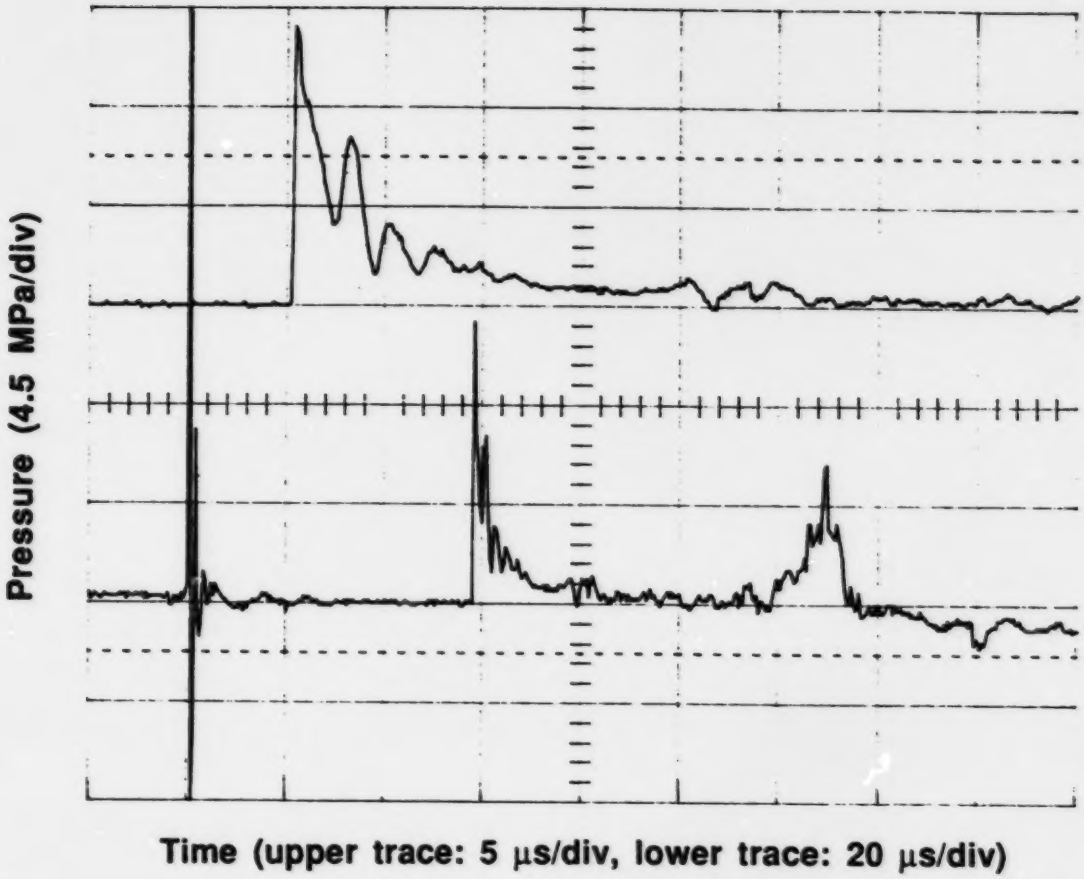

Fig. 3 Pressure at drop location from exploding wire trigger charged to 12 kV for apparatus #1. First spike on lower trace corresponds to electrical noise. Second pulse 60 μs later corresponds to arrival of shock wave at drop location. Upper trace shows expansion of initial shock wave (displaced to the left).

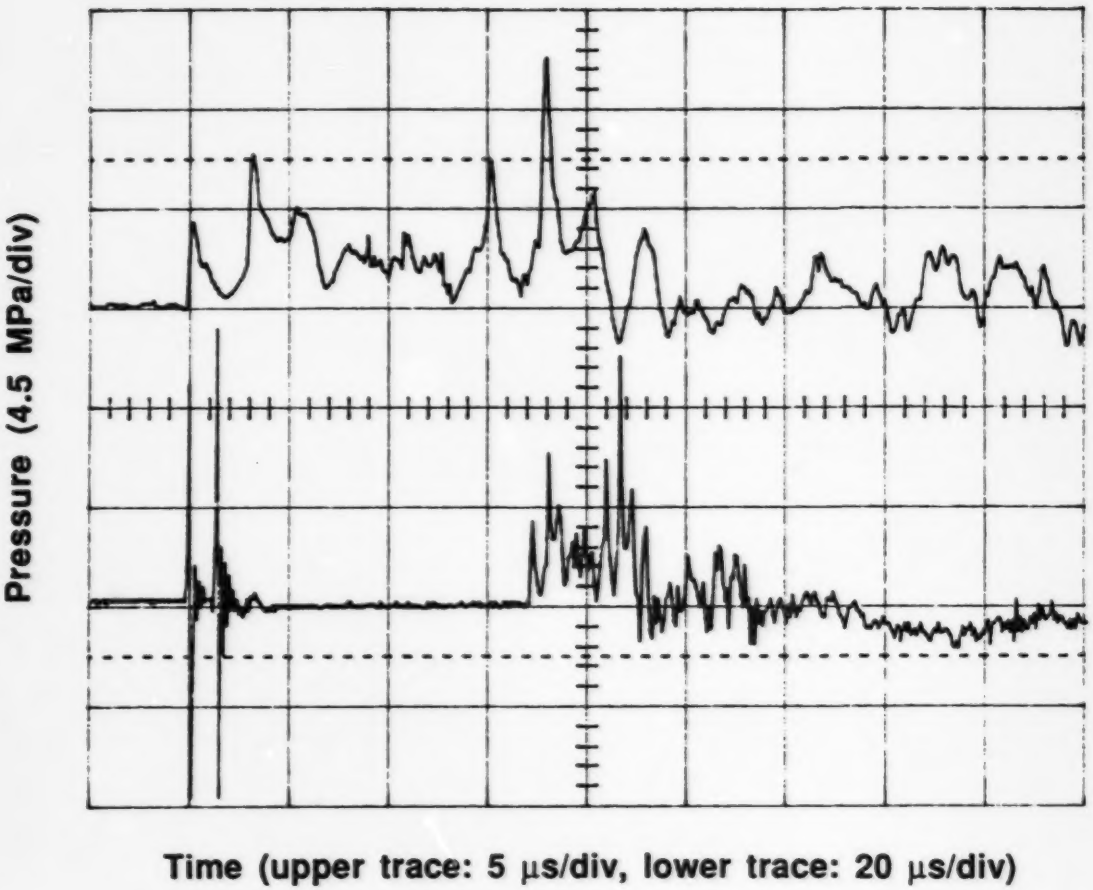

Fig. 4 Pressure at drop location from exploding wire trigger charges to 7 kV for apparatus #2. Upper trace shows expansion of lower trace.

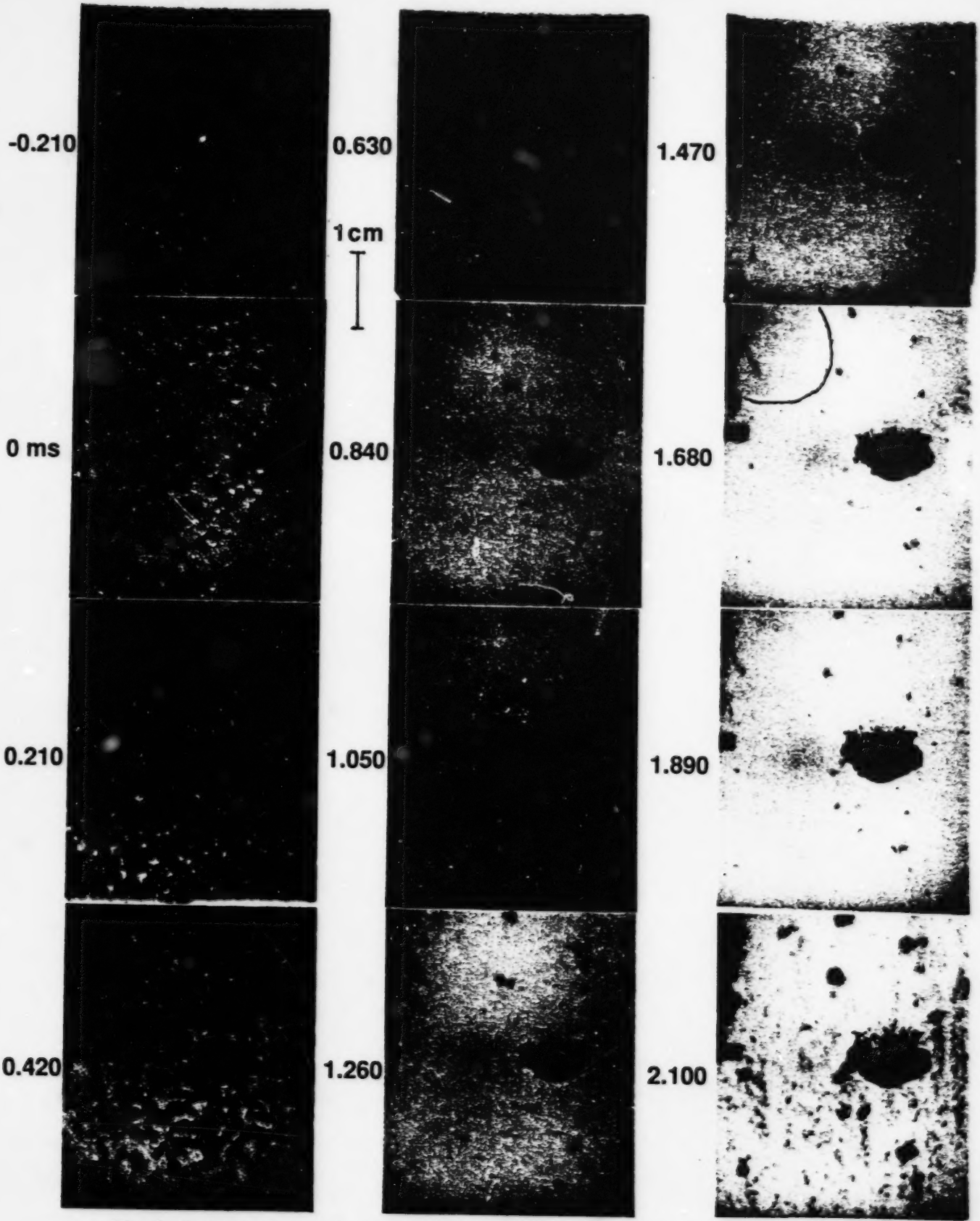

Fig. 5 Breakup of a cerrolow alloy drop (at 60°C) interacting with a 9.2 MPa blast wave. Shock moves from bottom to top.

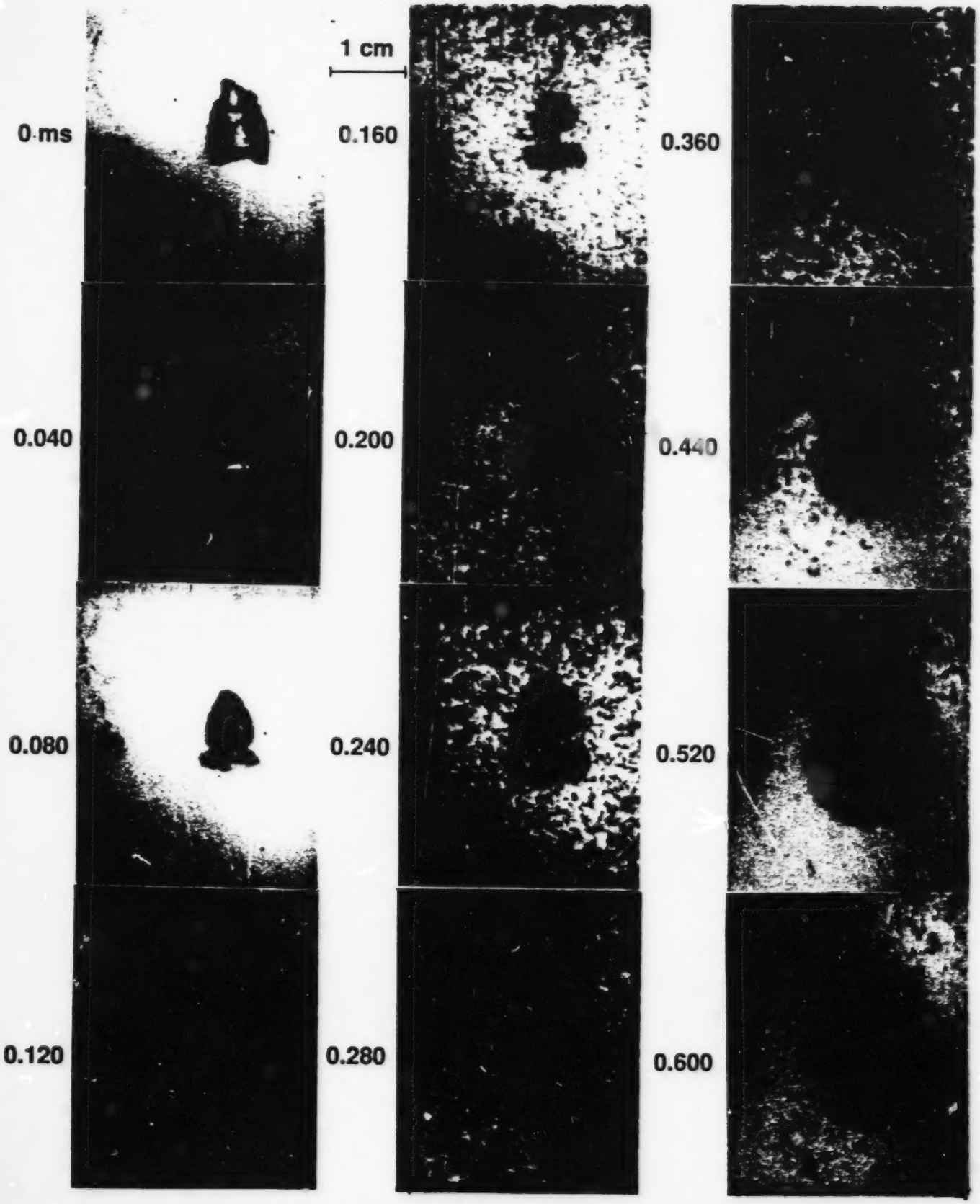

Fig. 6 Molten tin drop at 750°C interacting with a triggering shock with an overpressure of 6.0 MPa.

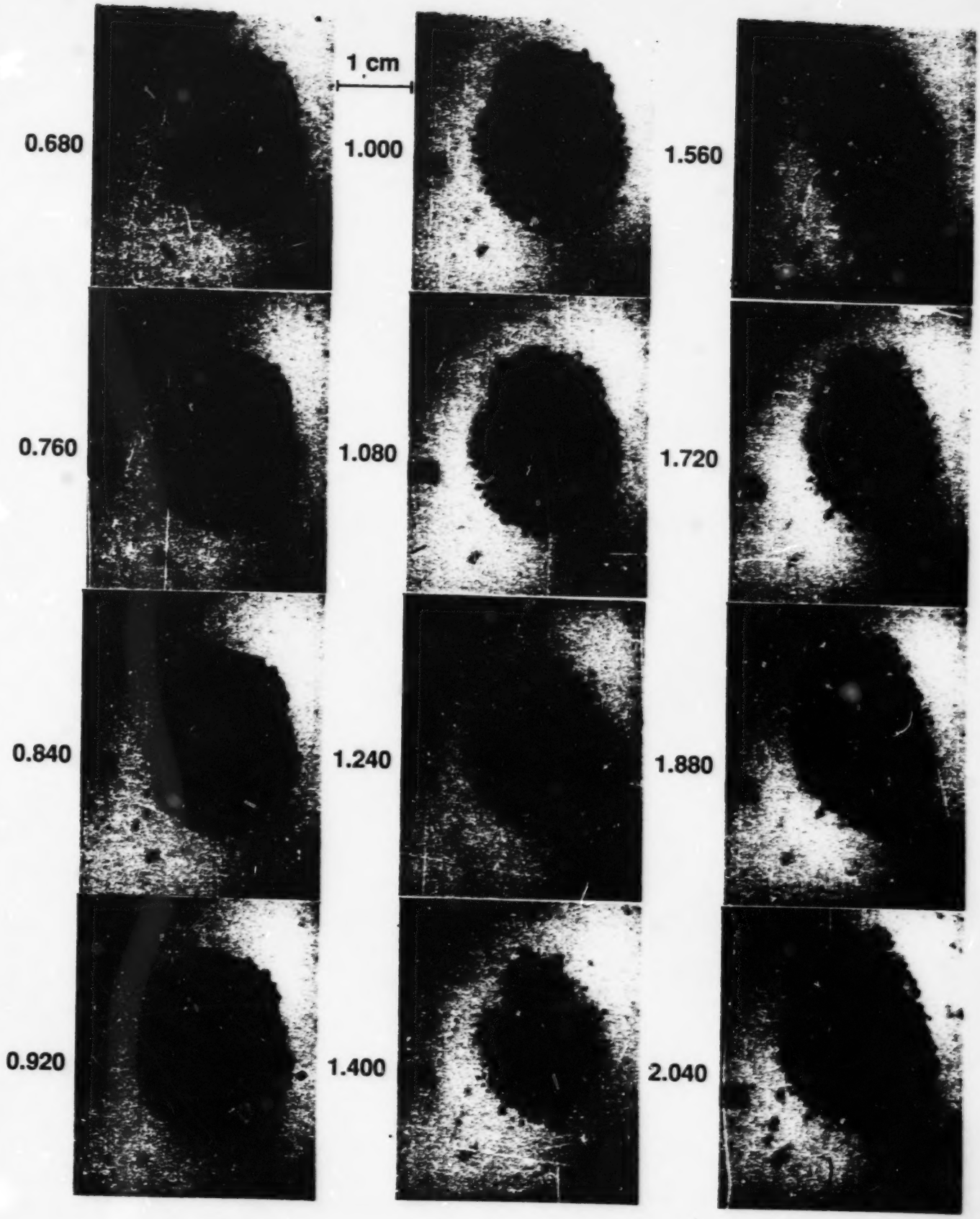

Fig. 6 continued

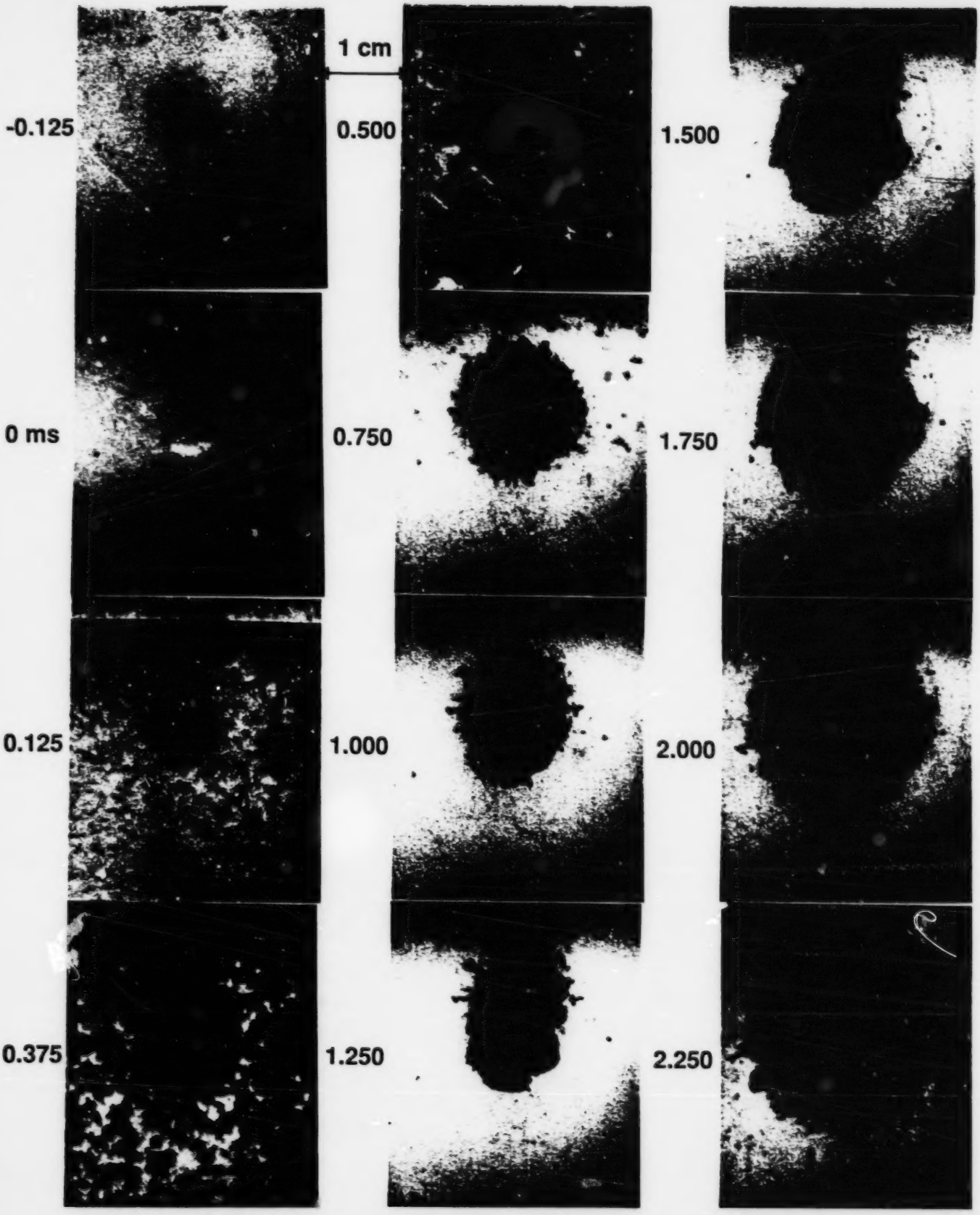

Fig. 7 Molten tin drop at 750°C interacting with a shock with pressure of 13.1 MPa. Dark object above drop is tip of funnel that serves to dislodge gas bag from drop.

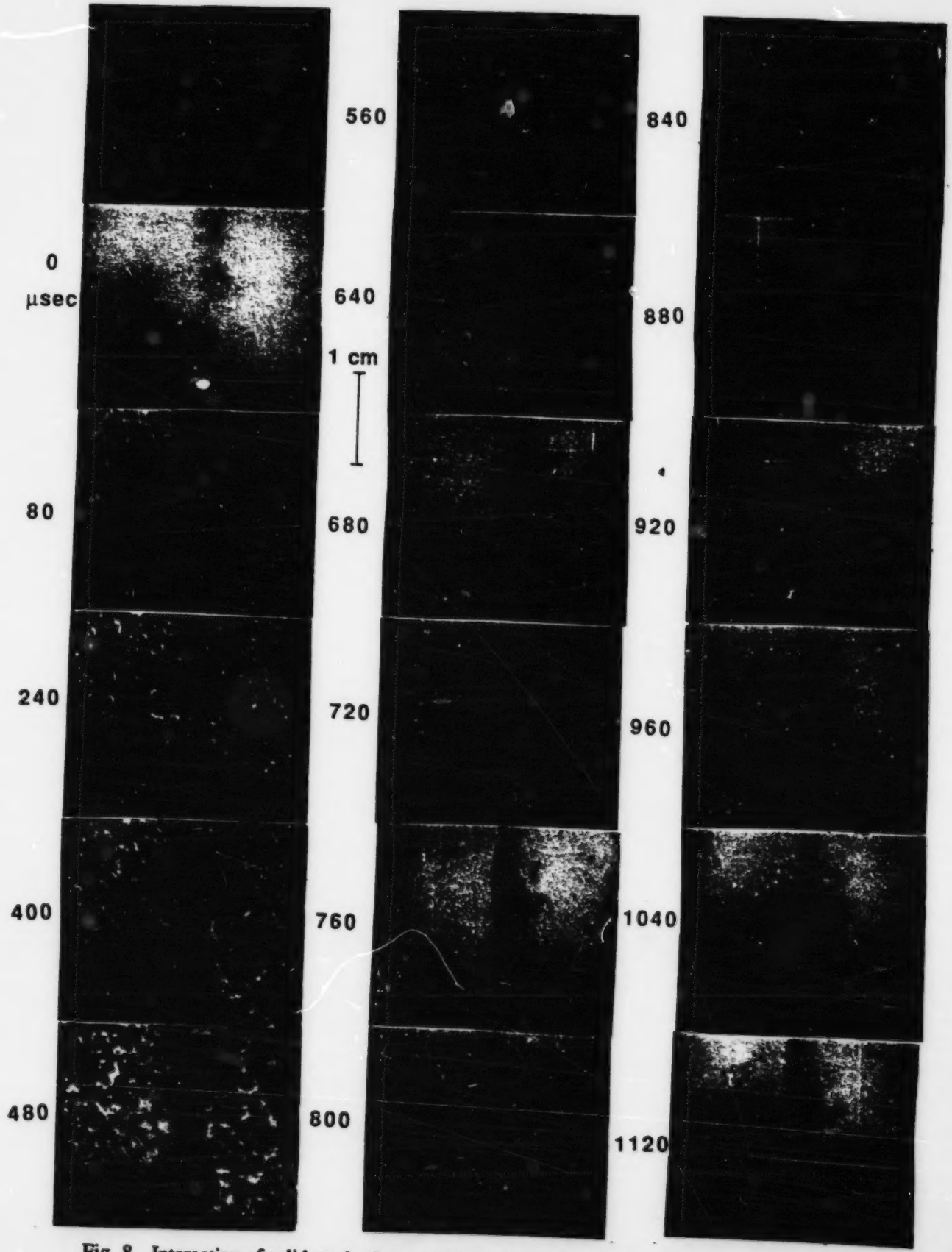

Fig. 8 Interaction of solid steel sphere at 750°C with a shock with a peak overpressure of 4.3 MPa.

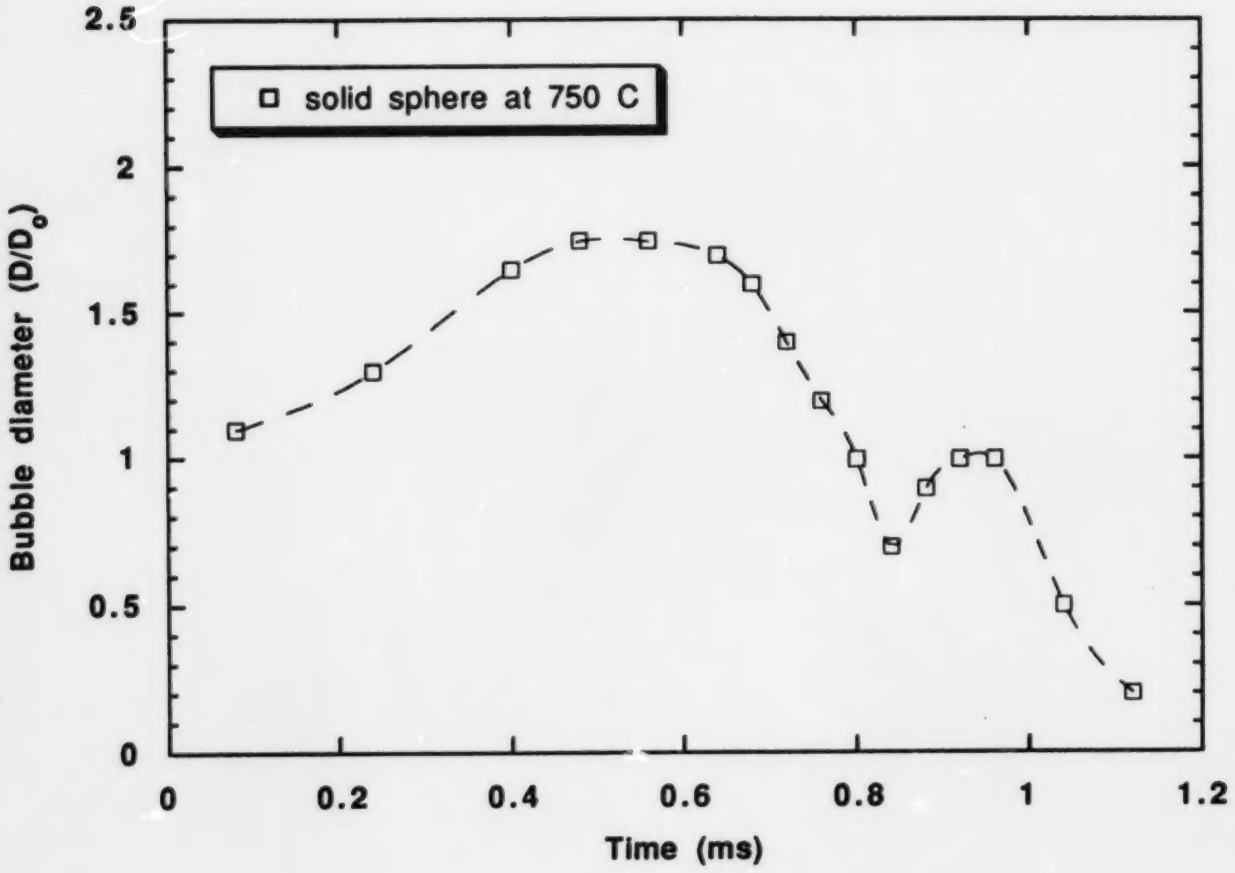

Fig. 9 Growth of steam bubble with time for the solid sphere shown in Fig. 8.

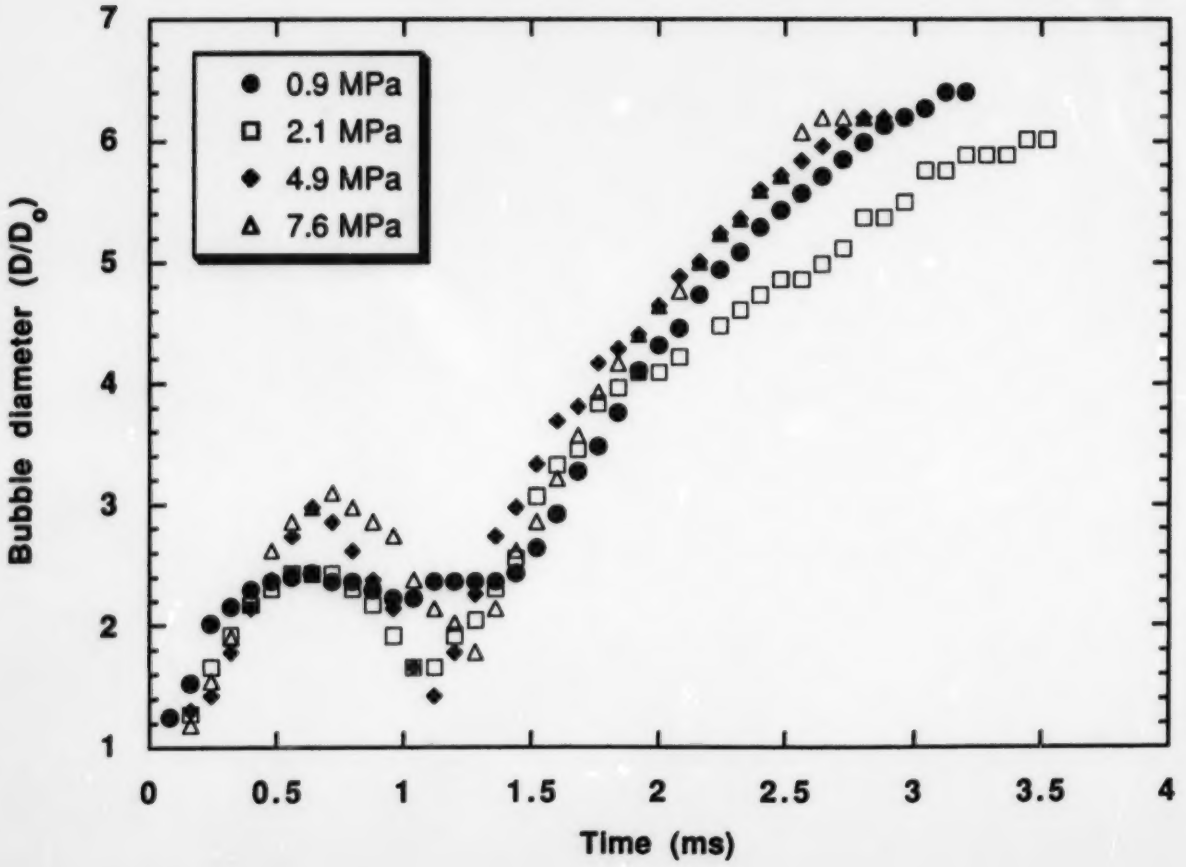

Fig. 10 Growth of steam bubble as a function of trigger pressure for 0.5 g tin drops at 750°C.

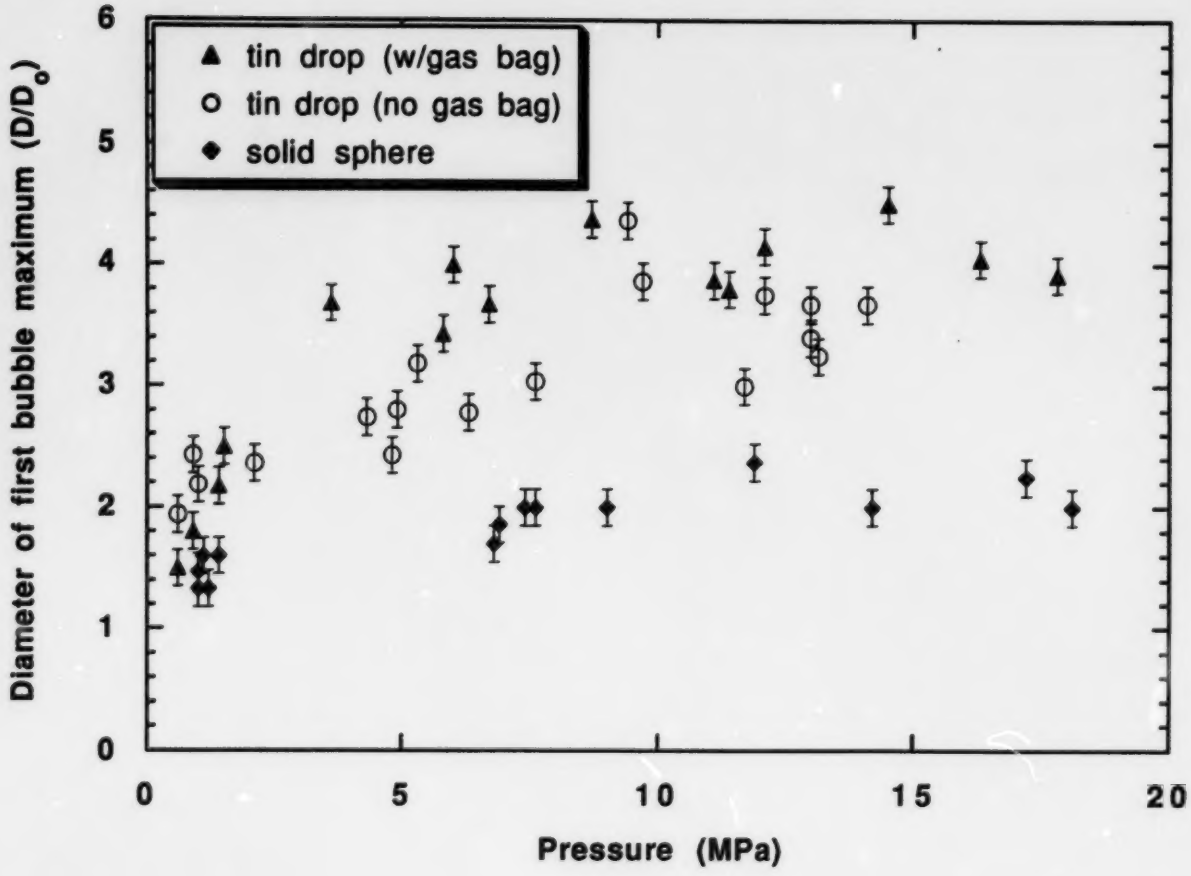

Fig. 11 Dependence of size of first bubble maximum with trigger pressure for molten tin drops and solid spheres, initially at 750°C.

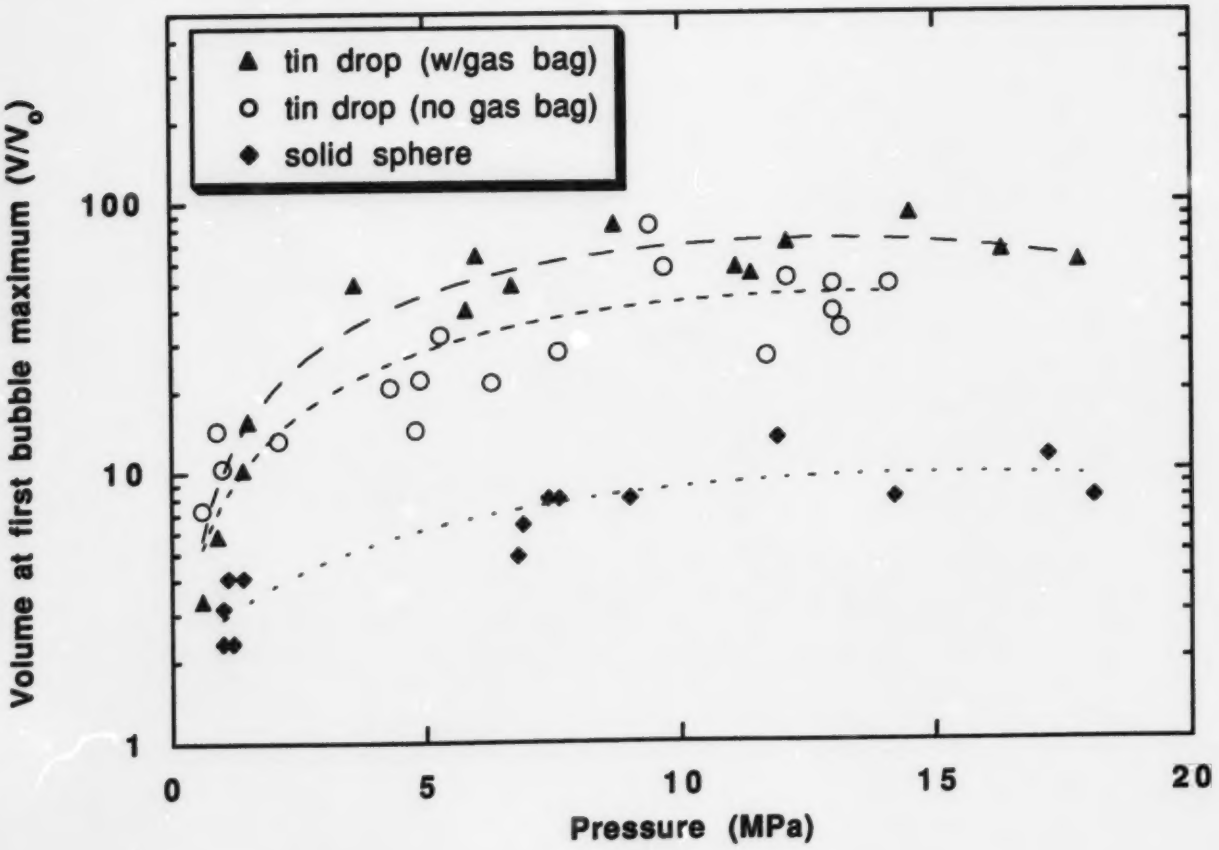

Fig. 12 Dependence of bubble volume at the first bubble maximum with trigger pressure for molten tin drops and solid spheres, initially at 750°C. Curves represent second order polynomial fits to the data.

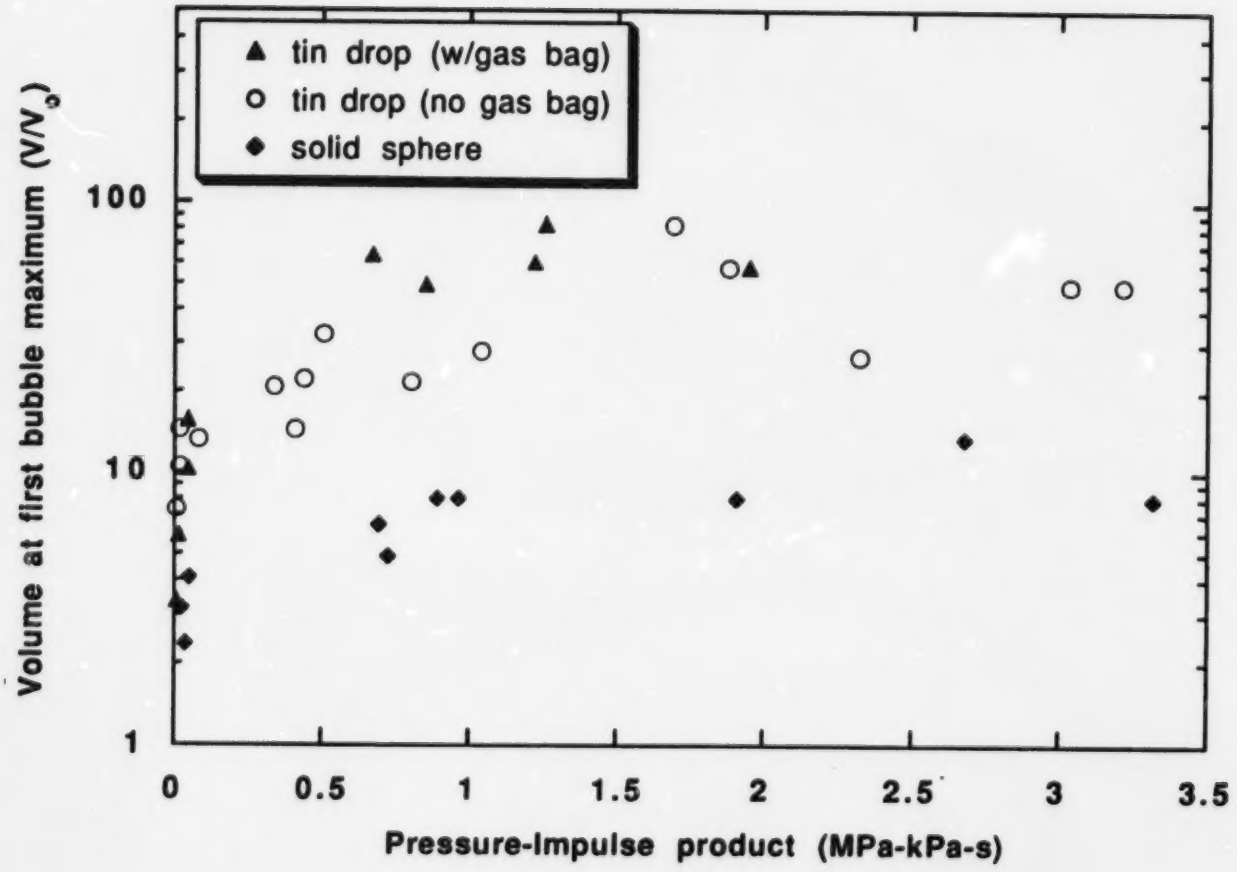

Fig. 13 Volume at the first bubble maximum as a function of PI product.

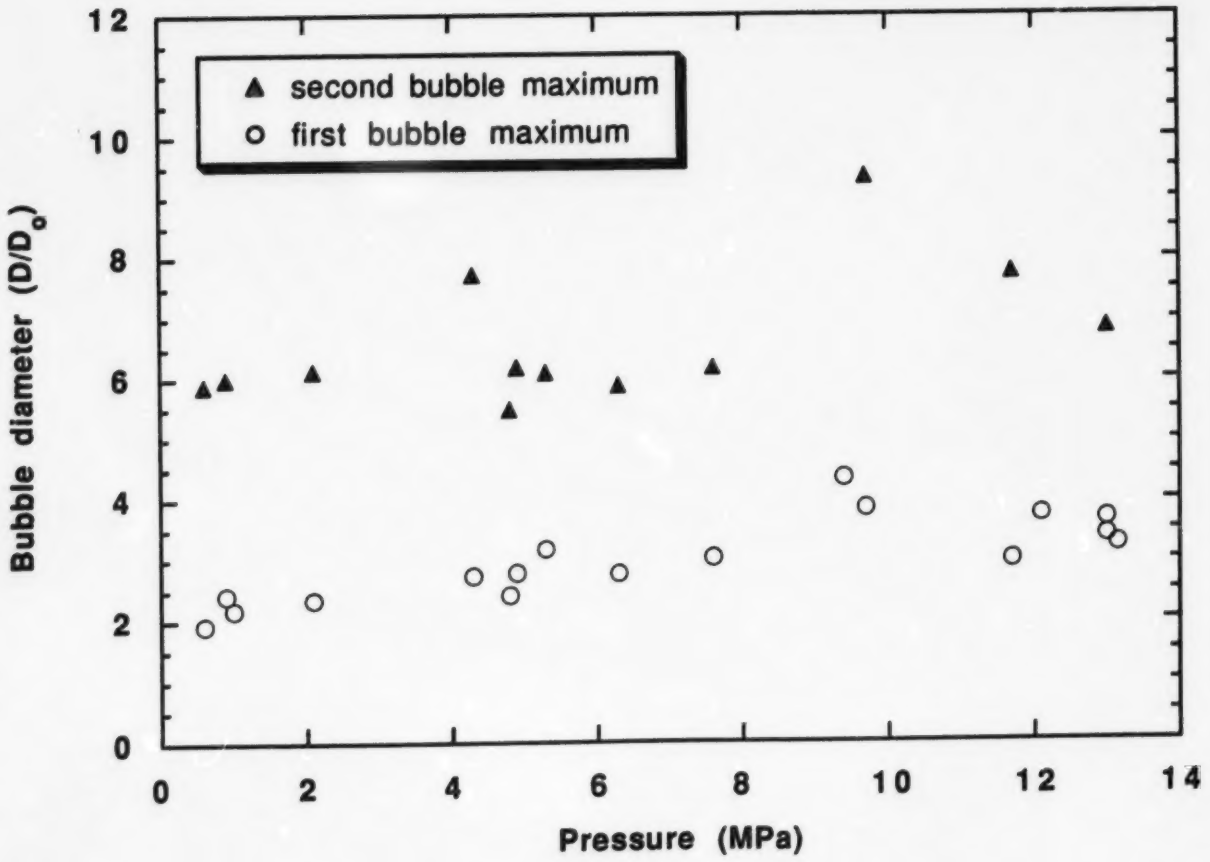

Fig. 14 Fist and second bubble maxima for 0.5 g tin drops at 750°C with no initial gas bag attached to drop.

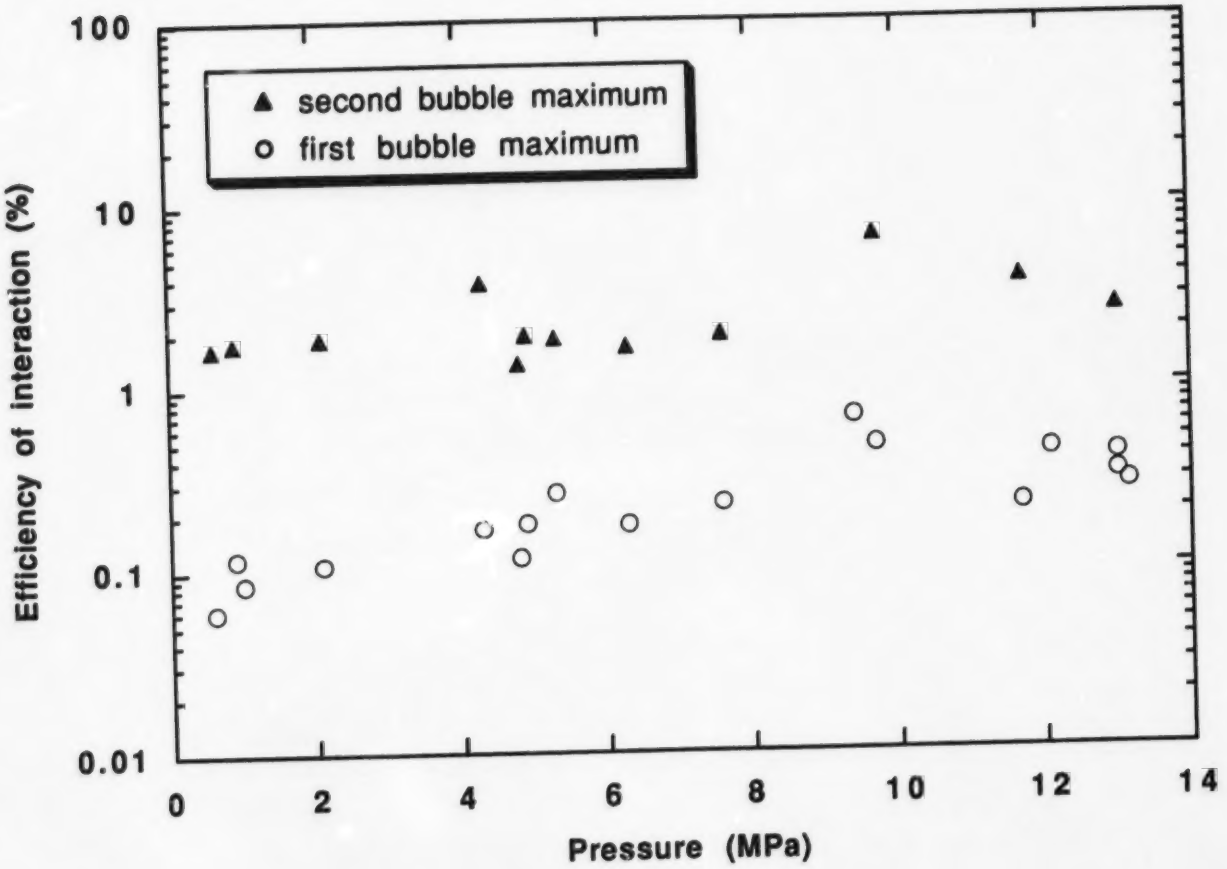

Fig. 15 Efficiency (or ratio of expansion work done and available thermal energy) for the first and second bubble maxima for 0.5 g tin drops at 750°C.

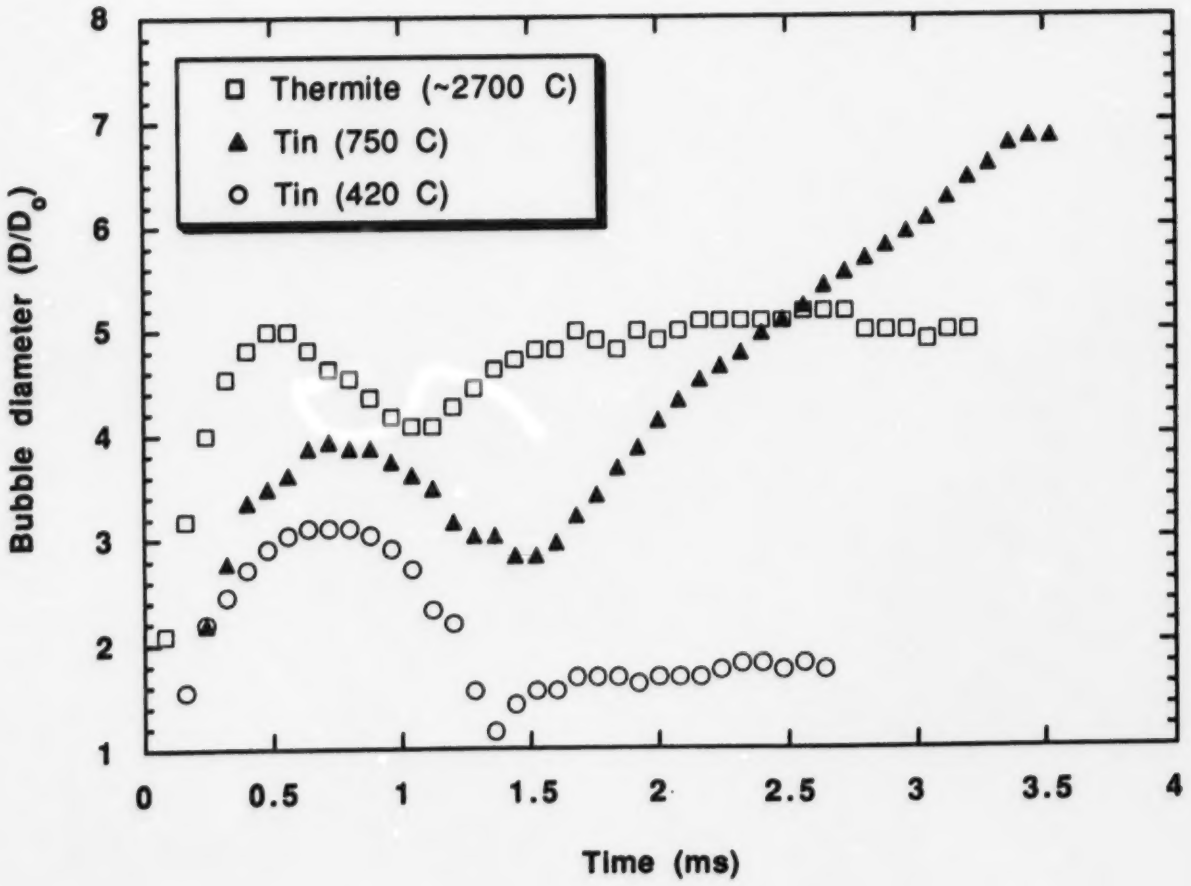

Fig. 16 Effect of thermal energy on the behavior of the steam explosion bubble. Mass of tin drops is 0.5 g and mass of thermite drop is about 0.7 g.

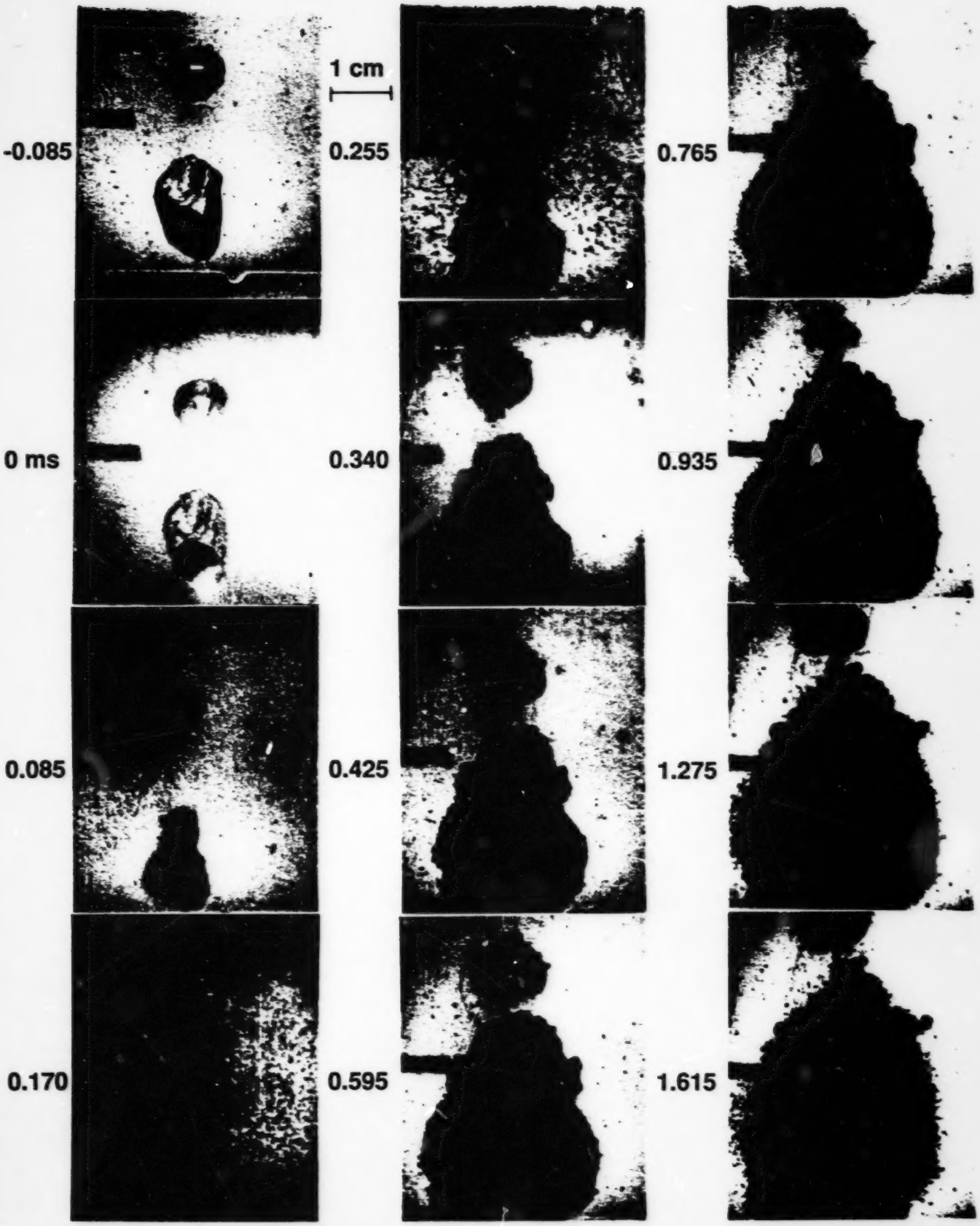

Fig. 17 Explosion of 0.7 g thermite drop (initially at a temperature of about 2700°C).

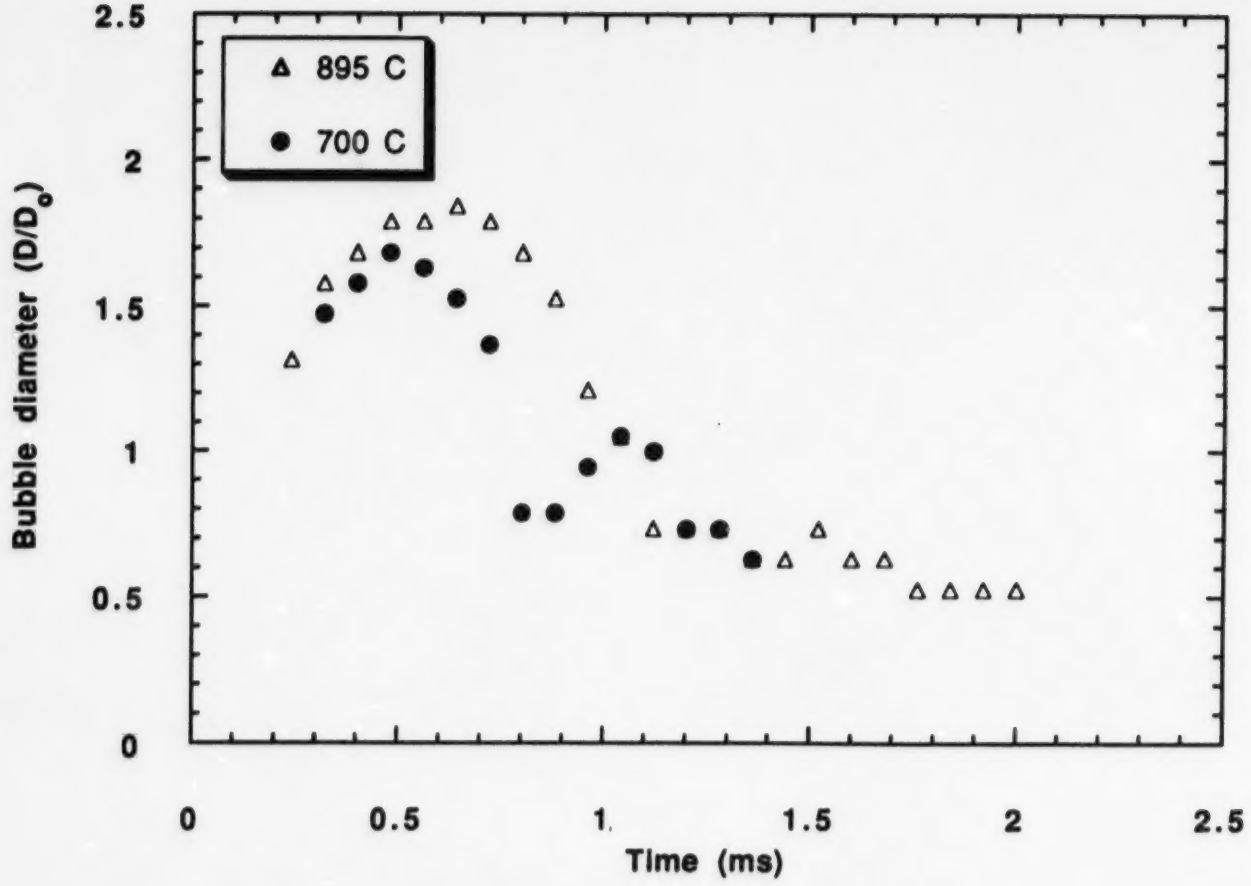

Fig. 18 Effect of temperature on the steam bubble generated during the interaction of a shock with a hot solid sphere.

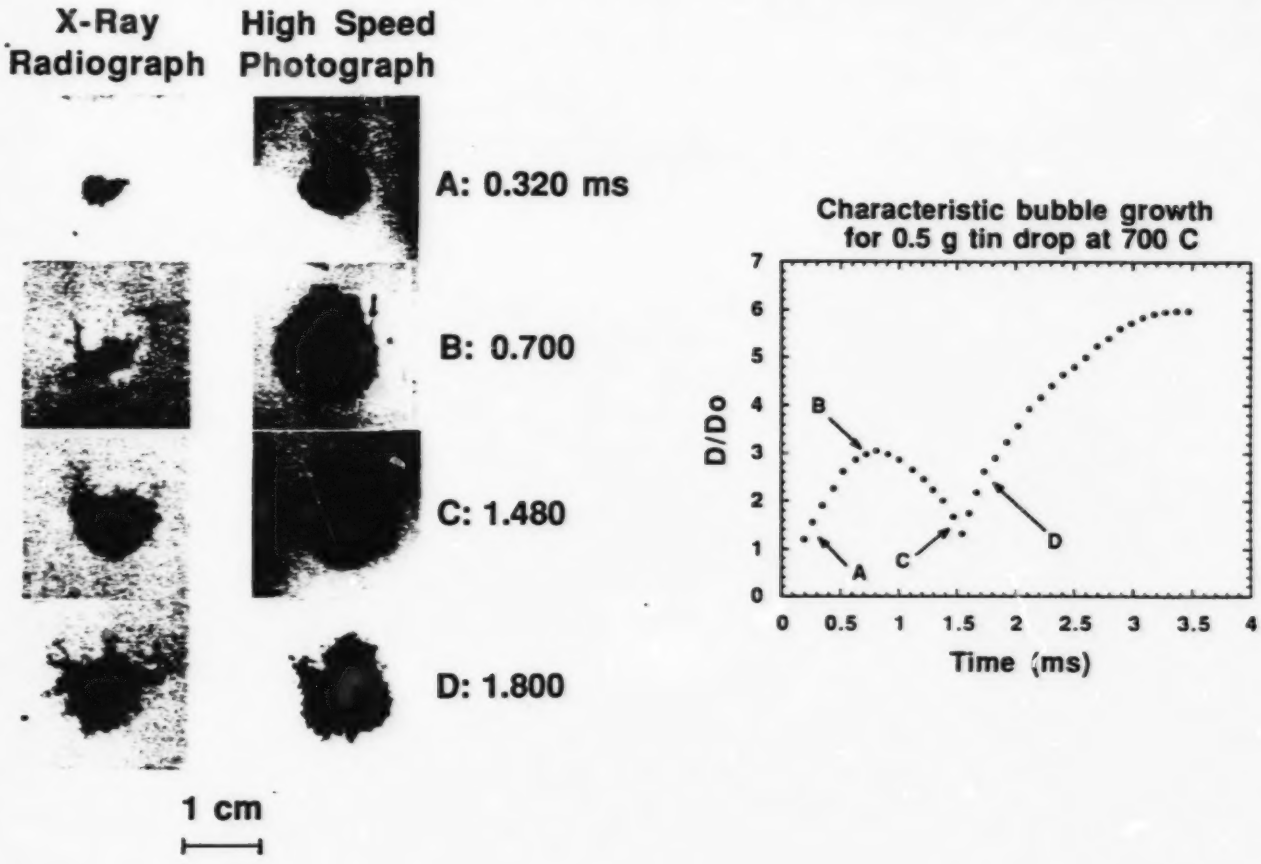

Fig. 19 Simultaneous x-ray and regular photographs of 0.5 g tin drops exploding. Trigger pressure varied from 5 to 6 MPa in each case.

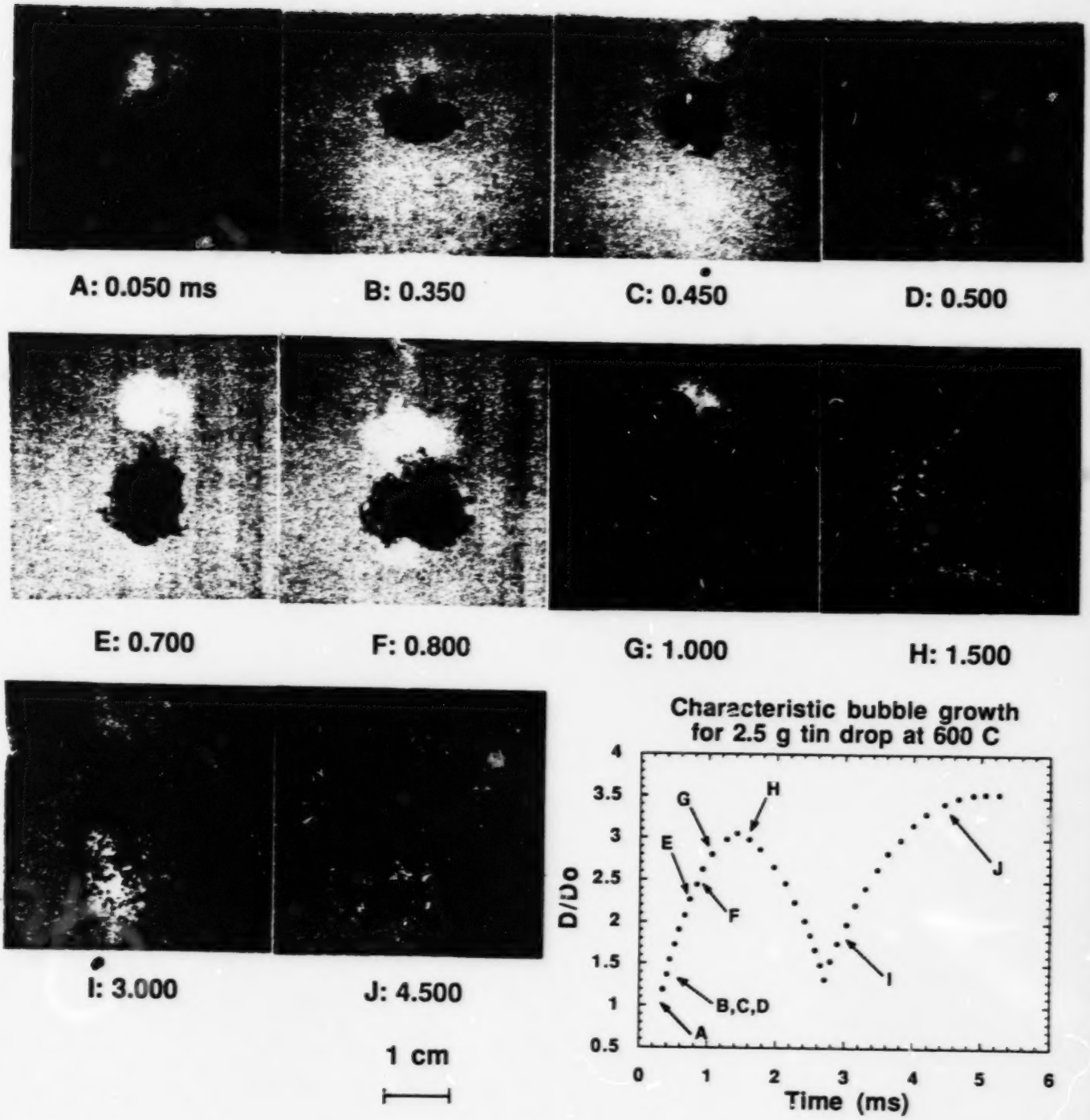

Fig. 20 Flash x-ray radiographs of steam explosion of 2.5 g tin drops (initially at 600°C). Note extensive fragmentation of tin during growth and collapse of first bubble.